EDGE DETECTION USING FRACTIONAL ORDER DIFFERENTIAL OPERATOR

Submitted towards the partial fulfillment of requirement for the award of degree of

Master of Engineering

in

Wireless Communication Engineering

Submitted by:

Sandeep Kaur

Roll No: 801363027

Under the guidance of:

Dr. Sanjay Kumar

Assistant Professor, ECED

ELECTRONICS AND COMMUNICATION ENGINEERING DEPARTMENT

THAPAR UNIVERSITY

(Established under the section 3 of UGC Act, 1956)

PATIALA – 147004 (PUNJAB)

July 2015

Certificate

I hereby declare that the work which is being presented in the thesis entitled, "**Edge Detection Using Fractional Order Differential Operator**" partial fulfillment of the requirement for the award of degree of Master of Engineering (E.C.E) at the Electronics and Communication Engineering Department of Thapar University, Patiala, is an authentic record of my own work carried out under the supervision of Dr. Sanjay Kumar, Assistant Professor, ECED. The matter presented in this thesis has not been submitted in any other University/Institute for the award of any other degree.

Date: 13 July 2015

Place: Thapar Uni. Patiala

Sandeep Kaur

Sandeep Kaur

Roll. No: 801363027

It is certified that the above statement made by the student is correct to the best of my knowledge and belief.

13/07/15

Dr. Sanjay Kumar
Assistant Professor
ECED,
Thapar University

Counter signed by:

Dr. Sanjay Sharma
Professor & Head
Thapar University
Patiala-147001

Dr. S. S. Bhatia
Dean of Academic Affairs
Thapar University
Patiala-147001

ACKNOWLEDGEMENT

This thesis is completed with prayer of many and love of my family and friends. However, there are few people that I would like to specially acknowledge and extend my heartfelt gratitude who have made the completion of this thesis possible. With the biggest contribution to this thesis; I would like to thank **Dr. Sanjay Kumar** who had given me his full support in guiding me with stimulating suggestions and encouragement to go ahead in all the time of the thesis.

I am also thankful to **Dr. Sanjay Sharma,** Head, Electronics and Communication Engineering Department, for providing us with the adequate infrastructure in carrying the work.

I am also thankful to **Dr. Amit K. Kohli**, P.G. Coordinator, Electronics and Communication Engineering department, for the motivation and inspiration that triggered me for the thesis.

At last but not the least my gratitude towards my parents, I would also like to thank God for not letting me down at a time of crisis and showing me the silver lining in the dark clouds.

SANDEEP KAUR

ABSTRACT

Edge detection has been widely used in the fields of Image processing, Computer vision, Feature vision n Feature extraction. Edges are detected in an image where the brightness of the image changes abruptly causing discontinuities in image brightness. Many mathematical tools aim at identifying these discontinuities also referred to as edges with in the image. The conventional operators such as Sobel, Robert, Prewitt are Discrete differential operators or often known as integer order differential operators. It was indicated that the edge detection methods operationally are an amalgamation of image smoothing and image differentiation in addition to a post-processing for edge labeling. It was indicated that the edge detection methods operationally are an amalgamation of image smoothing and image differentiation in addition to a post-processing for edge labeling. These integer order differential operators suffer from poor detection accuracy and noise immunity. In the presented work, a fractional order differential operator has been realised in combination of the integer order differential operators. The standard Lena image has been used for performing edge detection operations using both conventional as well as combination of conventional with fractional order differential operators. The improved operator can detect edges with high accuracy, good sharpness and with more detail. The fractional order differential operator has strong capacity to reduce noise than integer order differential operators.

Table of Contents

List of Figures

Page No.

List of Tables

Chapter 1

Introduction

1. Introduction

1.1 Image

An image is a two dimensional function which is represented as $f(x, y)$ in spatial domain. An image is basically digitized from a recorded image. Image is digitized by converting the continuous into digital form by the sampling and quantization processes. Intensity of the image is sampled by sampling process at discrete grid on some particular locations. A grid is the sampling resolution of the image. In sampling coordinate values are digitized. Sampled values are analog or continuous which are the values of intensity brightness converted into discrete form corresponds to each sample of brightness value. Brightness ranges from black to white through gray. Pixel or picture element is a digitized sample obtained by using sampling and quantization processes. Quantization basically digitized the amplitude values.

Image is denoted as $f(x, y)$ where x are the columns ranging from (0….N-1) and y defines the rows ranging from (0….M-1). N and M are total number of columns and rows respectively. Intensity values of image are directly proportional to the energy which is radiated by the physical processes such as optical or photographic sensors. For this $f(x, y)$ must be finite and non-zero. Function $f(x, y)$ is characterized by two components, illumination and reflectance. These are denoted as $i(x, y)$ and $r(x, y)$ respectively. Product of these two components formed the $f(x, y)$ as [1] :-

$$f(x, y) = i(x, y)r(x, y) \qquad (1.1)$$

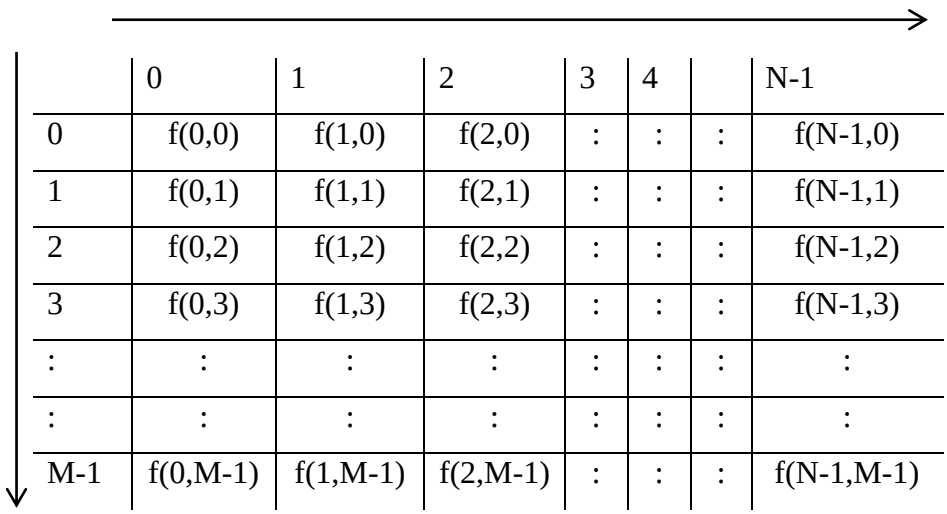

	0	1	2	3	4		N-1
0	f(0,0)	f(1,0)	f(2,0)	:	:	:	f(N-1,0)
1	f(0,1)	f(1,1)	f(2,1)	:	:	:	f(N-1,1)
2	f(0,2)	f(1,2)	f(2,2)	:	:	:	f(N-1,2)
3	f(0,3)	f(1,3)	f(2,3)	:	:	:	f(N-1,3)
:	:	:	:	:	:	:	:
:	:	:	:	:	:	:	:
M-1	f(0,M-1)	f(1,M-1)	f(2,M-1)	:	:	:	f(N-1,M-1)

Figure 1.1 Image Matrices [1]

Spatial resolution is defined as pixel per unit distance and lines per unit distance. It is the smallest distinct detail in image. It is a measure that how closely the lines are fixed in an image. Intensity resolution is defined as the smallest changes in intensity levels. It is given as an integer of power two:-

$$L = 2^k \tag{1.2}$$

where L is the number of intensity levels. It is depend on quantizing hardware considerations and storage. 2^k Intensity levels defines that image is of k-bit. For instance if an image has 512 discrete intensity values, it is called a 9-bit image.

Image is degraded by several factors during digitization process. When image is not sampled at the rate of twice than original image at highest spatial frequency then there occurs spatial aliasing. There is no method to control highest spatial frequency in natural scenes. Image is also degraded due to blurring which is caused by aperture. The third one is due to quantization because it represents infinite values of original image to finite values. So intensity values are not accurate. The fourth major factor is multiplicative and additive noise which produced by quantization devices which become the reason to thermal effects generally known as Gaussian noise.

If image is multi-spectrum or colored it is digitized in three planes red, green and blue. This image is called true color image because all the colors can be obtained from there three colors .RGB color space is a standard color space which is used to detect and generate colored lights. Other color space derivatives are also used for this purpose. The most common used derivative color space is the saturation, brightness and hue. The hue component controls the color spectrum, saturation describes that how washed color is with white and brightness controls the brightness of colors.

1.2 Pixels

The word pixel made up by the combination of two words 'pix' and 'el'. 'Pix' means picture and 'el' means elements. These are the smallest elements present in two dimensional grid which represent an image. These are represented by using dots or squares.Each sample of original image represents a pixel. So more number of samples provide accurate formation of original image. Each pixel has intensity which is variable. Pixels where the intensity of image changes suddenly called edge pixels. Edges are formed by joining these edge pixels. Edge pixels are detected by using edge detectors. When the intensity of pixels is much higher or lower than the intensity of background on either side of line is then it formed a line.

A pixel p has four horizontal and vertical neighbors at coordinate (x, y). These are given as:-

$$(x+1, y), (x-1, y), (x, y+1), (x, y-1) \tag{1.3}$$

	(x-1,y)	
(x,y-1)	(x, y)	(x,y+1)
	(x+1,y)	

Figure 1.2 Horizontal and Vertical Neighbors $N_4(p)$ of p [1]

These pixels are denoted as $N_4(p)$ and are known as 4-neighbors of p. If (x, y) is at the border of the image then some of its neighbor pixels lie outside the digital image.

An image also has four of diagonal neighbor of p which is at coordinates :-

$$(x+1, y+1), (x+1, y-1), (x-1, y+1), (x-1, y-1) \quad (1.4)$$

(x-1,y-1)		(x-1,y+1)
	(x, y)	
(x+1,y-1)		(x+1,y+1)

Figure 1.3 Diagonal neighbors $N_D(p)$ of p [1]

These are denoted by $N_D(p)$. Combination of $N_D(p)$ and $N_4(p)$ is called 8-neighbors of p. it is denoted by $N_g(p)$.

(x-1,y-1)	(x-1,y)	(x-1,y+1)
(x,y-1)	(x, y)	(x,y+1)
(x+1,y-1)	(x-1,y)	(x+1,y+1)

Figure 1.4 8-neighbors $N_g(p)$ of p [1]

To find the properties of a particular region within the image connectivity is used. In segmentation process, thresholding is used to differentiate between the backgrounds and object points. During this process a threshold value has set. If the value of x and y is greater than threshold value points belongs to the object. If value of x and y is lower than threshold then points will belong to the background. Object pixel assigns value 1 and represents white pixel where background points assign value o and represent black color.

1.3 Edges

Edges are defined as abrupt discontinuities in intensity of image. The change of intensity is so sudden that it forms like boundaries between different planes. Edges represent the difference of colors, patterns and outline of shape or texture. They are used to find corresponding points from number of images which are of same scene. Edge detection is defines as mathematical methods which are used to identify the points at which brightness of image changes abruptly. These points where brightness changes sharply are known as edges [2].

Edges provide the information about scene object due to the photometrical or geometrical variations. Physical edges are produced due to the variations in coordination, depth of scene surfaces, illumination and reflectance [2]. As intensity of image is proportional to scene radiance, physical edges are represented by variations in intensity function of image.

There are mainly three types of edges which are steps, lines and junctions. From physical edges, step edges are produced when an object hides another object or when there is shadow on surface. It happens when two regions have different but constant gray scale. Gray level discontinuity occurs at the step edges and these points are localized at the variation points. Gradient of intensity function is used to find these points. At first order derivative, step edges are placed at the positive maxima or negative minima or at second order derivative are zero-crossing [2].

For better results consider combination of multiple inflection points. Double step edge is used most commonly. These are of two types: the staircase and the pulse. The line edges are produced when two objects are in contact which have mutual illumination or when a thin object is placed over the background. Line edges are defines as local boundaries in intensity function of image. Lines correspond to confined extremes of image. These are localized as local maxima of the laplacian, or local maxima of gray level variance and zero-crossings of first derivative [2]. These types of edges are used in remote sensing images for example for the detection of rivers and roads.

A junction edge is defines as a point where two or more edges are joint together. A physical corner is produced when junction of two or more physical edges meet. A junction edge produced due to illumination effects or closure in which an edge blocks

another edge. Junction can be localized in many ways: for instance a point with large variations in the direction of gradient, a zero-crossing of the laplacian near elliptic extremes or with high curvature, or a point with high curvature. The edges can be classified as viewpoint dependent or viewpoint independent which are taken from a 2D image of a 3D scene. A viewpoint independent edge usually reflects characteristic properties of the 3D objects where viewpoint dependent edge reflects the geometry of the scene.

In binary images edges can be defined as the black pixels with one nearest white neighbor. Blurry edges are formed by the imperfections or problems happened during the image acquisition or sampling. These blurry edges seem like ramp profile. The slope of ramp is inversely proportional to the blurriness. Thickness of the ramp defines the length of ramp. Sharp edges are thin and blurred edges are thick. It is observed that first derivative is zero when intensity is constant and positive along the ramp. Second derivative is positive along dark side of edge and negative along the light side of the edge. It is zero outside and along the ramp. So first derivative gives the information about the presence of the edge at some points and second order derivatives are used to extract some secondary information.

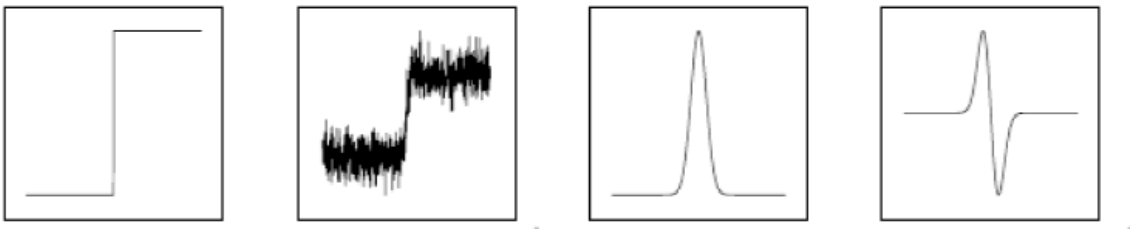

(a) (b) (c) (d)

Figure 1.5 - Profile of (a) Ideal Step Edge (b) Smoothed Step Edge Corrupted By Noise (c) First-Order Derivative (d) Second-Order Derivative of the Smoothed Step Edge Corrupted By Noise [2]

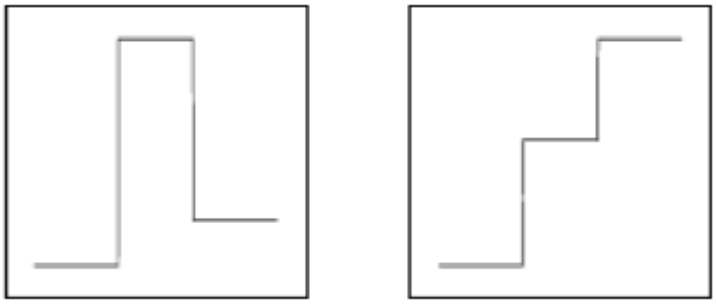

Figure 1.6 - Profile of Pulse (Left) and Staircase (Right) Step Edges [2]

1.4 Edge Detectors

Edge detection is a terminology which corresponds to the algorithms that are used to identify edges in an image. It deals with the areas of feature extraction or feature selection in an image. Edge detectors have input a digital image while the output is edge map. This edge maps explicit information about the strength and position as well as their orientation [2].

According to technical point of view, edge detection methods classified into two groups: search based and zero-crossing based [2]. In search based methods edges are detects first by computing their edge strength, such as gradient's magnitude of image intensity function. After that it searches its local maxima in the direction of gradient, direction which matches with edge profile. The zero-crossing based methods it search for zero-crossings in second order derivative to compute edges.

In point of conceptual view, edge detection methods are grouped into two categories: contextual and non-contextual approaches [2]. In the non-contextual methods it has no prior knowledge about the scene and edges. These are flexible that they are not limited to particular images. They perform the local processing on neighboring pixels. Contextual methods have priori about the edges and scene. They work accurately in precise context. They are used for general-purpose applications. Generally, contextual edge detectors are familiarizing to some particular applications that always work with images having same scene or objects.

The edge detection methods include three operations: differentiation, labeling and smoothing. Differentiation corresponds to extract the desired derivatives of image. Smoothing is used to reduce noise and normalizing numerical differentiation. Labeling is used to increase signal to noise ratio (SNR) and localizing the edges. It increases the SNR

by suppressing the false edges. Although labeling is the last stage but the order in which smoothing and differentiation is done, depends on their properties. Smoothing and differentiation of image is recognized only by filtering the image with differentiation of smoothing filter.

1.5 Different types of Noise in Image Processing

Noise in image is defines as random variations in brightness or color information in image [3]. Generally it is an electronic noise. It is produced by digital camera, sensor or circuitry of a scanner. Image noise is also initiate in the film grain and by an ideal photon detector in the form of unavoidable shot noise. Image noise is undesirable quantity that gives the false and unnecessary information.

The range of magnitude of image noise undetectable points on digital image that is taken in good light, radio astronomical and topical that is completely noise. Small amount of information is obtained by sophisticated process.

1.5.1 Gaussian Noise

It is a statistical noise which having probability density function equal to the normal distribution function. This is also known as Gaussian distribution. In other words these are the values that are taken by noise on Gaussian distributed [4].

The probability density function Υ of a Gaussian random variable x is given as:

$$\Upsilon_G(x) = \frac{1}{\sigma\sqrt{2\Pi}} e^{\frac{-(x-\mu)^2}{2\sigma^2}} \tag{1.5}$$

where x represents the grey level, σ the standard deviation and μ represents men value. A special case where values at any pair are statistically independent (uncorrelated) and identically distributed are known as White Gaussian Noise.

In digital images Gaussian noise occurred during acquisition. For instance, sensor noise originated by poor illumination and high temperature, and/or transmission. Gaussian noise can be decreased by using spatial filtering. This operation performed

when there is blurring of edges and details as outcome. This happens because of blocking of high frequencies. Conventional spatial filtering includes median filtering, mean filtering and Gaussian smoothing.

1.5.2 Salt and Pepper Noise

Salt and pepper noise presents itself as presence of white and black pixels. This kind of noise sometimes seen on images. For the reduction of this kind of noise median filter or morphological filters are used. Sometimes fat-tail distributed or impulsive noise is known as salt and pepper noise. An image having salt and pepper noise has dark pixels in bright regions and bright pixels in dark regions. This noise is occurred by analog to digital conversion errors, or bit errors during transmission. This kind of noise is reduced by using interpolating around bright/dark pixels or by using dark frame subtraction [4].

1.5.3 Shot Noise

From an image sensor, the central noise in the darker parts of the image is due to fluctuations of statistical quantum, i.e. at a given exposure the changes in the number of photons sensed. This noise is also called photon shot noise. The noises at different pixels are independent to each other. This noise has root mean square value proportional to the root of the image intensity. These noises follow Poisson distribution [5].

As well as photon shot noise, there is another shot noise by dark leakage current in image sensor. This noise is known as dark current shot noise or dark shot noise. At hot pixels dark current is at its maximum in the image sensor. The hot pixels and variable dark charge of normal pixels is subtracted off. It leaves only random component or shot noise of leakage. If the subtraction operation not performed, and if the coverage time is long enough that hot pixel charge go beyond the linear charge capacity, the noise will not be only shot noise but more than that, and hot pixels give the impression of salt and pepper noise.

1.5.4 Quantization Noise or Uniform Noise

This kind of noise is formed due to quantizing of pixels of detected image to a number of discrete levels. It is known as quantization noise. It follows the uniform distribution. It is signal dependent. Sometimes it becomes signal independent when other noise sources are big enough that produced dithering [6].

1.6 Smoothing

Noise in images is reduced by using smoothing operation [2]. Noise in image is referred as the points that do not match with the real scene. Noise is inevitable in image. Sampling noise or quantization noise produced when a real scene is transferring into limited pixels and limited colors. Noise in image creates problems in edge detection and localization process. Image smoothing has advantage that it reduces noise and confirms strong edge detection. But it also has disadvantage that it during this operation there is loss of some information which degrades edge boundaries. So there have to keep a trade-off between noise reduction and loss of information. When apply differentiation, it creates ill-posed in edge detection algorithms in the sense that the uniqueness, stability, and existence of solution cannot be guaranteed. Instability over the high frequency noise in image is another major problem. By using the regularization process we can convert ill-posed problem into well-posed problem and can get the existence of its uniqueness and solution. Regularization is characterization of the search for an optimal filter that forms the required additional constraints. These constraints concern the trade-off between preservation of edges during edge detection and noise reduction. So another aim of smoothing is Regularization of the numerical computation.

Image smoothing provides an optimal filter that negotiates between the reduction of noise and maintenance of image structure along with keeping the edge detection algorithms regular. Although this optimal filter guarantees this compromise, there is another challenge that is parameter adjustment. In image processing optimal filters have free parameter known as scale. So tuning the exact scale for filter is major challenge. These filters are described both in spatial and frequency domain. These filters are classified as linear filters and non-linear filters. Non-linear filters are more successful than linear filters as they remove certain kind of noise effectively while preserving the

edges. But non-linear filters are complex than linear filters. So linear filters are most commonly used because of their simplicity. There are three types of low- pass linear filters are used: support-limited filters, band-limited filters and filters with minimal uncertainty.

1.6.1 Smoothing Linear Filter

In this filter ever pixel value of an image is replaced by average of intensity levels in neighborhood pixels of x and y. This is done by using the filter mask [1].

1/9	1/9	1/9
1/9	1/9	1/9
1/9	1/9	1/9

Figure 1.7 Averaging Filter [1]

$$g(x,y) = \frac{1}{9}\sum_{i=-1}^{1}\sum_{j=-1}^{1} f(x+i, y+j) \qquad (1.6)$$

Here $f(x,y)$ is the original image and $g(x,y)$ is the output image. When this operation is performed output image is blurred image. This happens due to the averaging of all pixels in the neighborhood. Output image is smoothed image means it has blurred effect. All the sharp edges of image are replaced by blurring edges. To avoid the blurring effect another kind of filter is used which is known as weighted average filter [1].

1/16	2/16	1/16
2/16	4/16	2/16
1/16	2/16	1/16

Figure 1.8 Weighted Averaging Filter [1]

$$g(x,y)=\frac{1}{16}\sum_{i=-1}^{1}\sum_{j=-1}^{1}W_{i,j}\,f(x+i,y+j) \tag{1.7}$$

While performing this operation as doing average, weighting every pixel in the neighborhood by corresponding coefficients is also performed. This kind of filter is known as weighted average filter. Blurring effect is reduced by weighted averaging filter.

The final result of weighted averaging filter is:

$$g(x,y)=\frac{\sum_{i=-a}^{a}\sum_{j=-b}^{b}W_{i,j}\,f(x+i,y+j)}{\sum_{i=-a}^{a}\sum_{j=-b}^{b}W_{i,j}} \tag{1.8}$$

Here the mask size is $M\times N$. Where M is the number of rows in image and N is the number of columns in the image

$$M=2a+1 \tag{1.9}$$

$$N=2a+1. \tag{1.10}$$

By increasing the mask size image becomes more smoothed and blurred. During this operation noise is reduced but at the cost of blurring effect.

1.6.2 Non-Linear Filter

This filter depends upon the ordering of the pixel values in the neighborhood of points under consideration. So it choose the values which are in the neighbor of x and y. Then order these intensity values in a particular order. Based on this order select the points which are placed on center region (x, y) in processed image g(x, y), by using this process we get the processed image. This processing is done using the order statistics filter. This kind of filter is known as median filter [1].

1.7 Fractional Calculus

Fractional calculus is a branch of mathematic field that rises out of traditional definitions of calculus derivative and integral operators in much the same way Fractional exponents are a process of exponents with integer value. The Fractional calculus is an abstraction of traditional calculus that leads to similar tools and concepts, but with a much large-scale appropriateness. In September 30th, 1695 L'. Hopital wrote to Leibniz

and asked him about a particular notation which he had used in his paper for the nth-derivative of the linear function f(x)= x, $\frac{D^n f(x)}{D^n x}$. He asked that would it be possible to perform half-differentiating of function x. Then Leibniz replied that it leads to a paradox, from which useful consequences will be drawn one day [7]. The paradoxical aspects are because of the fact that there are several different ways of simplifying the differentiation operator to non-integer powers, having in equivalent results.

Euler, Fourier and Laplace are among the many that dabbled with mathematical consequences and Fractional calculus [8]. Many initiate, by using their own methodology and notation, definitions that suitable for the concept of non-integer order integral or derivative. Fractional calculus is considered in different definitions and Fractional differential of some special kind of function is given. The most famous definitions in the world of Fractional calculus are Grunwald-Letnikov (G-L) and Riemann-Liouville (R-L) definitions. The most classic definition of Riemann-Liouville is given by Caputo in order to solve his fractional order differential equations by using integer order initial conditions.

Some of the reasons why fractional calculus is catching on are [9]

- Most biological signals have spectra that do not increase or decrease with multiples of 20dB/decade. This occurs, for instance, with speech, ECG, music etc. the electronic line is a channel with such properties.
- The fractional Brownian motion (fBm) is most famous and has attracted attention because of their importance in many practical systems. Although there are many ways for synthesis or analysis of such signals but fractional derivatives are proven most efficient.
- According to Curie law current in an insulator increases proportionally to negative power of time. This indicate to the known ‘super capacitors’ that have impedance of the form $\frac{1}{\omega^{\alpha}}$ where 0 <a< 1. Constant Phase Elements description is used by electrochemists for over 60 years. ‘Fractance’, a new terminology

indicates impedance with fractional order response. Many of the rules for design of controllers and filters are known as these devices available commercially.

There is growing and long list of practical applications for the increased power of fractional calculus. These include [9]

- Acoustics
- Robotics
- Control
- Electromagnetism
- Edge detection
- Thermal engineering
- Viscoelasticity

1.8 Objective of Thesis

- To compare the performance of different type of edge detection operator from the point of view of various performance metric parameters.
- To establish the analytical model of fractional differential mask based on different definitions of fractional order calculus approach.
- To establish the edge detection operation utilizing the proposed fractional differential mask and compare this mask operator with the conventional operators.

1.9 Organization of Thesis

This thesis consists of six chapters that are given below:

1. Introduction, it consists of introduction to image, pixels, edges and fractional calculus.
2. Literature review, study of research papers of related field in sequence has been discussed.

3. Edge detection of image, it consists of edge detection techniques and conventional operators are discussed.

4. The Fractional Differentiation, in this G-L based fractional differentiation is discussed, then a physical and geometric meaning of fractional differentiation is studied and its edge detection capability is discussed.

5. Fractional order differential operator, in this chapter edge detection by using an Improved Fractional Differential is discussed.

6. Results and Discussions, this chapter consists of all the results simulated using MATLAB-2007. The fractional differential operator is applied to Lena image and edge detected images are analyzed using various parameters.

7. Conclusion and future scope, this chapter consists whole work has been concluded on the basis of results obtained and future scope.

Chapter 2

Literature Survey

In this present chapter, a brief account has been put forth of the available literature that has been studied extensively.

M. Juneja (2009) *et. al* [10] In this paper they described comparative analysis of various Image Edge Detection methods. The evidence for the best detector type is judged by studying the edge maps relative to each other through statistical evaluation. Upon this evaluation, an edge detection method can be employed to characterize edges to represent the image for further analysis and implementation. It has been shown that the Canny's edge detection algorithm performs better than all these operators under almost all scenarios.

In this paper, authors analyzed the behavior of zero-crossing operators and gradient operator on the capability of edge detection for images. The methods are applied to the whole image. No specific texture or shape is specified. The objective is to investigate the effect of the various methods applied in finding a representation for the image under study. On visual perception, it can be shown clearly that the Sobel, Prewitt, and Roberts provide low quality edge maps relative to the others.

N. Kanopoulos (1988) *et. al* [11] in this paper the authors concentrate on design and implementation of a monolithic image edge detection filter using the Sobel operators. The chip architecture is highly pipelined in performing the computations of gradient magnitude and direction for the output image samples. The function of the chip has been demonstrated with a prototype system that is performing image edge detection in real time. Even though the design of the Sobel chip is not especially ambitious relative to currently available advanced technologies, the design is of sufficient complexity to illustrate the considerable potential for quick turnaround implementation of special-purpose image processing algorithms on a single chip using a silicon compiler. The

design approach also demonstrates that architectural provisions can be taken to match algorithms to hardware, making possible implementation of an image processing operation on a single chip, using mainly random logic primitives and yet a structured design environment.

P. H. Eichel (1990) *et. al* [12] in this paper they proposed an operator based on the sample variance of a group of pixels, which exhibits three unique properties: freedom from a predefined shape, low computational complexity and a rigorous stochastic formulation. The utility of the latter property in applying detection theoretic principles to the task of edge detection and in theoretical predictions of experimental performance measures is demonstrated. The new operator is compared with other common edge operators on natural scenes.

In this paper they showed that the sample variance operator is useful for detecting intensity edges in images. Under the hypothesis of additive, Gaussian distributed i.i.d. noise; the operator's probability density function was shown to be very accurately approximated by a Gaussian density. This allows the use of a likelihood ratio test to analytically determine a decision threshold for the operator. They proved a theorem concerning the prediction of the optimum decision threshold for the Pratt figure of merit. The theorem states that under suitable conditions the optimum threshold may be predicted as a function of the signal-to-noise ratio and further that the resulting merit value may also be determined.

E. A. El-Kwae, (1998) *et. al* [13] in this paper they developed an algorithm that detects well-localized, unfragmented, thin edges in medical images based on optimization of edge configurations using a genetic algorithm (GA). Several enhancements were added to improve the performance of the algorithm over a traditional GA. The GA was compared to the simulated annealing (SA) approach using ideal and actual medical images from different modalities including magnetic resonance imaging (MRI), computed tomography (CT), and ultrasound. Results for different medical image modalities are promising and encourage further investigation to improve the accuracy and experiment with different cost functions and genetic operators.

In this paper, the optimization on cost evaluations and transformations defined by Tan et al. [14] [15], where SA was used for the optimization. They extended the bit string chromosome of the traditional GA to a bit-array chromosome, which conforms closely to a logical edge representation. They introduced problem space reduction with dependent regions. To increase the performance of the traditional GA, they added reduced surrogate crossover, ranking selection, dynamic operator rates, and stochastic evaluation on the operators.

X. Wang (2007*) et. al* [16] has described Laplacian operator which is a second derivative operator often used in edge detection. Compared with the first derivative-based edge detectors such as Sobel operator, the Laplacian operator may yield better results in edge localization. Unfortunately, the Laplacian operator is very sensitive to noise. In this paper, based on the Laplacian operator, a model is introduced for making some edge detectors. Also, the optimal threshold is introduced for obtaining a Maximum a Posteriori (MAP) estimate of edges. In this paper, based on the Laplacian operator, two edge detectors named OED and MED are introduced. Also, the optimal threshold is introduced by a MAP estimate. Examples show that the proposed edge detectors are effective both in edge detection and noise smoothing. How to make better edge detector with the EDM is an interesting problem.

H. WECHSLER, (1977) *et. al* [17] in this paper they proposed new edge detection technique for digital image processing is presented. The technique is viewed as a low-level operator in the context of the more complex problem that of scene analysis and a conceptual comparison with some previous edge detectors is done. The new edge detection technique has been implemented and its results are compared with two other edge detection techniques using the same kind of pictures as input data. Spurious edges can be eliminated by using a combination of global and local thresholding and by taking into consideration the characteristics of the edge as found by the finite differences. The novelty of the proposed method consists in using the finite difference approach for identifying candidates for local edge elements and in the way the thinning operation is performed.

N.H.Hamid, (2009) *et. al* [18] has proposed design and implementation of gradient based edge detection algorithm using of Sobel operator. An image is captured by a CMOS camera and converted into grayscale to obtain image intensity for edge detection. The Sobel edge detection operator is controlled by Finite State Machine (FSM) which executes a matrix area gradient operation to determine the level of variance through different of pixels and display the result on a monitor. The whole process is performed in the hardware level and implemented on an Altera field programmable gate array platform. This design can be operated with 27 MHz clock frequency. The above mentioned performance was achieved with good proper set up of timing analysis. Improvement can be made for the future work with design of dedicated co-processor for the Sobel edge detection algorithm.

C. Fan, (2010) *et. al* [19] In this paper they described several typical edge detection operators in digital image processing are theoretically analyzed, and are used for road edge detection. By comparing the simulation results of road edge detection, the better road test results can be gained when using Sobel operator and Prewitt operator. At the same time, the application environment for each operator is provided.

In this paper, the application environments of the operators are also gained in the process of road edge detection. However, none of them is a method of absolute advantage. Some edge detection algorithms have high detection accuracy, but anti-noise performances are poor. Others can solve the problem about poor anti-noise performances, but detection accuracies are not well. Therefore, each edge detection algorithm has different types of defects while solving certain problems. So, it has been one of image processing purpose to search simple algorithm which can better solve the coordination problem between the edge detection accuracy and the anti-noise performance.

R. Harinarayan, (2011) *et. al* [20] in this paper they proposed edge detection algorithms based on FPGA architecture. The implementation of edge detection algorithms on a field programmable gate array (FPGA) is having advantage of using large memory and embedded multipliers. FPGAs are providing a platform for processing real time algorithms on application-specific hardware with substantially higher performance than

programmable digital signal processors (DSPs). The proposed architecture can be used as a building block of a aerial imaging systems for navigation and for the pattern recognition. The hardware implementation results are presented for the Sobel and Prewitt operator. In this paper two different methodologies for the edge detection of aerial images are implemented on the FPGA. Lower requirements of the FPGA resources make this method easy to be integrated with the aerial surveillance instruments and automatic navigation equipments.

X. Hou1, (2012) *et. al* [21] In this paper authors discussed and evaluate the performance of different parameters, firstly Canny edge detection operator based on optimization algorithm is discussed which has advantages of large signal and noise ratio and high accuracy. Secondly, the welding image processing with Canny operator is described and for every step, detailed description and processing results are given. At last, canny operator edge detection results are projected to 2-d histogram. The histograms of projection results are compared with the qualified image histogram. When the similarity is higher than some threshold, we think that the welding is qualified. On the contrary, we consider the welding as disqualified one. On the base of above algorithm, the welding by robot is effectively detected. So automatic welding in the production line and automatic welding identification can be achieved.

V. V. Kishore, (2012) *et. al* [22] in this paper Morphology based Region of interest segmentation combined with watershed transform of DICOM lung image is performed and comparative analysis in noisy environment such as Gaussian, Salt & Pepper, Poisson and speckle is performed. The ROI lung area blood vessels and nodules from the major lung portion are extracted using different edge detection filters such as Average, Gaussian, Laplacian, Sobel, Prewitt, Unsharp and LoG in presence of noise. The results are helpful to study and analyses the influence of noise on the DICOM images while extracting region of interest and to know how effectively the operators are able to detect, overcoming the impact of different noise. The validity of the paper work is performed by applying the procedure on DICOM image with different noises. This makes easy way to

detect and study the ROI. This method can be used as an initial step for Computer Aided Diagnosis to evaluate the performance of various edge detecting methods.

D. Yadav, (2013) *et. al* [23] in this Paper they discussed several Digital Image Processing Techniques applied in edge feature extraction. Firstly, Linear filtering of Image is done is used to remove noises from the image collected. Secondly, some edge detection operators such as Sobel, Log edge detection, canny edge detection are analyzed and then according to the simulation results, the advantages and disadvantages of these edge detection operators are compared.

It is shown that the canny operator can obtain better edge feature. Finally, Edge detection is applied to find crack in a bone of a hand.Applies a 3x3 convolution filter row-wise in order to determine the gradient of the surrounding pixels. Pixel is a member of an edge if the intensity of it is greater than that of the members of its surrounding pixel. The operator of Canny detects edges by looking for the local maximums of the gradient of image. In this method the derivative of a Gaussian filter is used for of gradient. Log The operators of Laplacian of Gaussian (LOG) and the Zero-crossing detect edges by looking for zero crossings after filtering the original image with a Laplacian of Gaussian and a specific filter respectively.

Y. Ye, (2013) *et. al* [24] in this paper, a novel complex mask for the implementation of fractional differentiation is deduced. By the combination of fractional differentiation and integration, a new compound derivative is proposed, in which the fractional-order derivative mask is employed. The compound derivative, together with the complex mask, is applied to edge detection, forming a new edge detection operator. The performances of the compound derivative, in terms of detection effectiveness and noise immunity, are demonstrated through 1D example. Finally, quantitative analysis demonstrates that the new operator can outperform *Canny* operator. The 1D and 2D detection examples show that, without *Gaussian* smoothing, the performance of the new algorithm is promising. The new algorithm can balance detection accuracy and noise immunity through the tuning of α– β. High positioning accuracy and low positioning error manifest that the new algorithm has highly authentic edge locations with few missed edges and false

edges. Through the evaluations of execution time and memory footprint, the new algorithm demonstrates to be computationally efficient and memory economic.

D. Tian, (2014) *et. al* [25] this paper introduces a novel fractional-order gradient operator for medical image structure feature extraction. The proposed operator can be seen as generalization of the first-order Sobel operator based on the GL fractional derivative definition. The generalization goal is to utilize the frequency characteristic of the fractional derivative for extracting more structure feature details. A thresholding is set based on the average fractional-order gradient for marking the edge points, and then the image structure can be extracted. The fractional global operator can consider more neighboring information. Considering this characteristic, we generalize the traditional first-order Sobel edge detection operator to fractional-order for extracting image structure features. The novel operator has been validated on brain MR images and a cardiac ultrasound image with desirable performance.

A. Jain, (2014) *et. al* [26] in this paper they studied various edge detection methods and different kinds of operators using edge detection. The various edge detection techniques such as Robert, sobel, prewitt, canny are compared with each other. In end a new nature inspired algorithm has been proposed and compared with the traditional operators. We see that the number of edges detected are more when detected with the bio inspired algorithms. In this paper carried out the proposed algorithm on random pixel in the input images. Also the various traditional edge detection methods were compared with each other and with the optimization algorithm technique and a graph is plotted which shows that the proposed MFA technique gives the best results. Also results shows that the traditional operators uses masks and ignore the corner pixels.

G. N. Chaple, (2015) *et. al* [27] in this paper they presented comparisons of Robert, Prewitt, Sobel operators based edge detection techniques for real time uses. Edge detection algorithms are written with the help of hardware descriptive language VHDL. Xilinx ISE Design Suite-13 and MATLAB software platforms are used for simulation purpose. The FPGA supports high levels of parallel processing data flow structures that

are important for efficient designing of real time image processing algorithms. FPGAs can be a promising solution for real time image processing work. FPGA hardware utilization is less in Robert operator based edge detection as compare to Prewitt and Sobel operator. Edge detection efficiency of Sobel operator is better than Prewitt and Robert operator.

X. H. Chen, (2012) *et. al* [28] in this paper authors discussed how to use the advantages of fractional differential method to improve the shortcomings of Roberts. Firstly, both the Roberts and fractional differential theory are clearly explained respectively. Secondly, it discusses in detail the structures and parameters of 3*3 any order fractional differential mask on eight orientations. Lastly, it puts forward a new method based on combination fractional differential and Roberts operator. This paper intends to apply a newly mathematic approach to improve the edge detection methods based on the traditional integer order differential and achieves the better experimental results. It provides reference for the thin edge detection needed and also promotes the application of fractional differential.

C. Gao, (2014) *et. al* [29] in this paper authors proposed a new mask according to the development of the fractional differentiation and its applications in the modern signal processing, we improve the numerical calculation of fractional differentiation by Newton interpolation equation, and, the Newton Interpolation's Fractional Differentiation (NIFD). Then this new mask apply to image edge detection and can obtain the better edge information image. Experiments show that the NIFD operator has excellent edge detection capabilities and especially plays an important role in reducing the noise sensitivity.

Z.J. Hou, (2002) *et. al* [30] has proposed two classes of new edge detectors, DSC edge detector (DSCED) and DSC anti-noise edge detector (DSCANED) for the detection of multi scale edges. This paper introduces the discrete singular convolution (DSC) algorithm for edge detection .The DSCED is capable of extracting the fine details of images, whereas DSCANED is robust against noise. The combination of two classes of

DSC edge detectors provides an efficient an reliable approach to multi scale edge detection.

The performance of the proposed algorithm is compared with many other existing methods, such as the Sobel, Prewitt and Canny detectors. The performance of the proposed algorithm is compared with many other existing methods, such as the Sobel, Prewitt and Canny detectors. The Canny detector can be optimized with respect to the 4lter length and time–frequency localization, whereas, the DSC detector can be optimized with respect to one more parameter, , which plays the role of frequency selection. Experiments on a variety of images have been carried out with some selected DSC parameters, and the performance of DSC detectors is at least as good as that of the Canny detector.

Q. He, (2007) *et. al* [31] has proposed a new edge detection algorithm for Image
Corrupted by White-Gaussian noise that can reasonably consider White-Gaussian noise reduction and correct location of edge, and provides its specific arithmetic process .Finally, the comparison based on principle of new edge detection algorithm and classical edge detection operator is done, the experimental results indicate that the performance of new edge detection algorithm is better than that of classical edge detection operator. The new edge detection algorithm that this paper proposes, not only can overcome the deficiency of being sensitive to White-Gaussian noise, which exists in classical edge detection operator, but also ensures the continuity, integrity and accurate location of image's edge. Moreover, because the steps of new edge detection algorithm are compact, it is applicable to image's practicable processing.

Y. Zhang, (2010) *et. al* [32] in this paper they analyzed the fractional calculus's Riemann-Liouville definition and derives 1~2 order(n+2)×(n+2)fractional differential mask of digital image, including x positive direction, x negative direction, y positive direction, y negative direction, left upper diagonal, left lower diagonal, right upper diagonal and right lower diagonal. Based this mask, the experiments show that this fractional differential calculation can not only maintain the low frequency contour information in the smooth area, but also nonlinear enhance the high frequency edge and texture part in the image.

This paper deduces the fractional differential masks based on the classical Riemann-Liouville definition. When the fractional order is between 1 and 2, it can enhance the texture and edges in mutiscale by controlling the fractional order. In experiments, the fractional differential operator can not only preserve the low-frequency smoothing area, but also nonlinearly enhance the high-frequency part, texture and edges, and it is the numerical property of fractional differential. However with the increment of the size of the masks, the precision get higher, but the edges drift effect will appear.

Y. Pu, (2010) *et. al* [33] in this paper they implemented a class of fractional differential masks with high-precision. They discussed further the capability of multiscale fractional differential masks for texture enhancement. Experiments show that, for rich-grained digital image, the capability of nonlinearly enhancing complex texture details in smooth area by fractional differential-based approach appears obvious better than by traditional intergral-based algorithms. They proposed 6 fractional differential masks, then demonstrate the most efficient fractional mask by theoretic and experimental analyzing, and finally discuss the texture enhancement of multiscale fractional mask. Experiments on real data sets show that the fractional differential- based approach is obvious better than traditional integral differential-based algorithms when nonlinearly enhance comprehensive texture details in smooth area of texture-rich digital images.

J. Zhou, (2011) *et. al* [34] In this paper, according to the development of the fractional differentiation and its applications in the modern signal processing, we improve the numerical calculation of fractional differentiation by piecewise quadratic interpolation equation, that is, improved fractional differentiation, IFD for short, and propose a new corresponding operator, IFD operator. And they apply this new operator to image enhancement. Experiments show that, for texture-rich digital image, the capability of nonlinearly enhancing comprehensive texture details by IFD is very obvious. The particularity of IFD operator is that the derivative order between 0 and 3 favors enhancement selectivity, which expands the transition width of fractional differentiation order $0<v<1$. Experiments show that the IFD operator has excellent textural details enhancing capabilities for rich-grained digital images. And finally for quantity analysis,

from information entropy and average gradient, they both show that IFD operator can nonlinearly enhance comprehensive texture details.

D. Chen, (2013) *et. al* [35] has proposed an image enhancing method which is based on the non-local fractional order differential operator. The proposed enhancing method is able to make effective use of the whole image information and improve the enhancing performance of the image enhancing algorithm based on the local mask. A non-local fractional differential-based approach was proposed for image enhancement in this study, which includes the following contributions. Firstly, the matrix approximate method is extended to new version which is suitable for the image enhancement. Secondly, the effective non-local fractional order differential image enhancing method is proposed based on the improved matrix approximate method, which solves the problem of use of local fractional differential numerical approximate. Finally, a lot of experiments verify the validity of proposed method.

J. Scharcanski, (1997) *et. al* [36] in this paper they discussed an approach for detecting edges in color images. The proposed approach can easily accommodate concepts, such as multiscale edge detection, as well as the latest developments in vector order statistics for color image processing. A distinction between the proposed approach and previous approaches for color edge detection using vector order statistics is that, besides the edge magnitude, the local edge direction is also provided. The proposed edge detector is an extension to color images of concepts developed for grayscale images. It shows promising results, and we intend to further develop this approach by improving the accuracy of the edge location mechanism using color information and also extending this approach to include some of the recent advances in vector order filtering for color images.

H. Yang, (2010) *et. al* [37] in this paper authors proposed fractional differentiation and integration to obtain a new edge detection operator. The performances in terms of detection accuracy and noise immunity of the new operator are compared with those of the traditional operators through examples. The comparison shows that the new operator

is promising. The proposed YE&YANG operator eliminates the smoothing preprocessing and provides a new approach to tune the compromise between noise immunity and detection accuracy. The comparison with CANNY and CRONE operators in the experiments demonstrates the superiority of the proposed method. Extension of the proposed idea to a second-order derivative based edge detection scheme is ongoing.

M. Chakraborty, (2008) et .al [38] In this paper they performed an in-depth mathematical analysis the Grunwald-Letnikov definition in depth. Based or analysis, they presented a transformation scheme which will allow us to accurately analyze generalized fractional order systems in presence of significant quantities of random errors. Finally, by a simple experiment, demonstrate the high degree of robustness to noise offered by the said transformation and thus validate our scheme.

As an experimental validation of this thesis, they presented in the values of $D^{\alpha}e(t)$ for 5 different sets of randomlygenerated9 e(t) with α=1.5, 0.9, 0.3, –0.3, –0.9, –1.5. The amplitude of e (t) varies between –0.01 and 0.01. Length of memory L = 10 seconds. Sampling rate is once in 0.001seconds. In the light of section VI, we contend that, to minimize the effect of error, we must ensure that all the fractional differ integrals to be computed are fractional integrations rather than fractional differentiations. Using the modified set of simultaneous equations, in presence of the exact random error waveform (with its elements varying between –0.05 and 0.05) that was used for the experiment mentioned in section IV, we have a1 = 0.7992, a 2 = 0.4996, a 3 = 0.9996 as the estimates of the unknown parameters. The errors in estimating them are respectively 0.1000%, 0.0800% and 0.0400%. Comparing this result with that obtained under ideal conditions, at the end they conclude that proposed scheme successfully eliminates the effects of noise.

Chapter 3

Edge Detection

3.1 Introduction

Edge detection is a terminology in image processing that refers to algorithms which aim at identifying edges in an image. It is encountered in the areas of feature selection and feature extraction in Computer Vision. An edge detector accepts a digital image as input and produces an edge map as output. The edge map of some detectors includes explicit information about the position and strength of the edges and their orientation.

3.1.1 Mask

Mask is a filter. Concept of masking is also known as spatial filtering. Masking is also known as filtering. This concept deals with the filtering operation that is performed directly on the image.

Sample mask is shown below.

-1	0	1
-1	0	1
-1	0	1

Figure 3.1. Simple Mask

3.1.2 Filtering

The processing of filtering is also known as convolving a mask with an image. This process is same of convolution, so filter masks are also known as convolution masks. The general process of filtering and applying masks consists of moving the filter

mask from point to point in an image. At each point (x, y) of original image the response of filter is calculated by a predefined relationship. All the filter values are predefined and are standard.

3.1.3 Types of Filter

There are two types of filters. One is called as linear filter (smoothing filters) and other are called as frequency domain filters [1]. Filters are applied on image for multiple purposes. The most common uses are.

1. Filters are used for blurring and noise reduction.
2. Filters are used for edge detection and sharpness.

3.1.4 Blurring

Filters are most commonly used for blurring and for noise reduction. Blurring is used in preprocessing steps, such as removal of small details from an image prior to large object extraction. In blurring we simply blur an image [1]. An image looks sharper or more detailed if we are able to perceive all the objects and their shapes correctly in it. For example, an image with a face looks clear when we are able to identify eyes, ears, nose, lips forehead etc. very clear. This shape of an object is due to its edges. So in blurring, we simple reduce the edge content and make the transition from one color to other very smooth. You might have seen a blurred image when you zoom image when you zoom an image using pixel replication, and zooming factor is increased you saw as blurred image. This image also has less detail, but it is not true blurring. Because in zooming, you add new pixels to an image that increase the overall number of pixels of a normal image.

3.1.5 Sharpening

Sharpening is opposite to the blurring [1]. We reduce the edge content. So in order to increase the edge content in an image, we have to find edges first. After finding edges, we will add these edges on an image and thus image would have more edged and it would not look sharper.

3.2Image Edge Detection Techniques

3.2.1 Image Differentiation

The First and second orders of a derivative of an image are the most common in the edge direction methods. For instance, to detect step edges we can look for maxima of absolute value of the first derivative or zero crossings of the second derivative an image. This section reviews the required mathematical background to compute the differentiation of an image [39]. Consider $g(x,y)$ as a function defined in $R\times R\longrightarrow R$ that represents the image value. The first-order derivative of g can be calculated along a direction of r, using the partial derivatives of g along the main axis.

$$g_x=\frac{\delta g}{\delta x}, g_y=\frac{\delta g}{\delta y} \tag{3.1}$$

$$\frac{\delta g}{\delta r}=\frac{\delta g}{\delta x}\frac{\delta x}{\delta r}+\frac{\delta g}{\delta y}\frac{\delta y}{\delta r}=g_x\cos\phi+g_y\cos\phi \tag{3.2}$$

where ϕ is the angle formed between r and x axis. The gradient of g is a vector with the same direction as the maximum directional derivative, and its magnitude and direction are defined

$$\left|\Delta g\ \right|=\sqrt{g_x^2+g_y^2} \tag{3.3}$$

$$\varphi_v=\arctan\left(\frac{g_y}{g_x}\right) \tag{3.4}$$

According to definition, we can say that edge points may be located by the maxima of the module of gradient, and the direction of edge contour is orthogonal to the direction of gradient. The edge detection methods based on the gradient are directional, since they give their maximum response when they are aligned with the orthogonal direction of the edges contour.

Edge detection based on second order derivatives is frequently performed using one of two operators: the second derivative along the direction of gradient or the Laplacian [39]. The second derivative of along the direction of gradient or the Laplacian. The second derivative of g along the gradient direction is related with the derivatives along the axes x and y in the following way:

$$\frac{\partial^2 g}{\partial r^2} = \frac{g_x^2 + 2g_x g_y g_{xy} + g_y^2 g_{xy}}{g_x^2 + g_y^2} \tag{3.5}$$

$$g_{xx} = \frac{\partial^2 x}{\partial r^2}, g_{yy} = \frac{\partial^2 g}{\partial x^2}, g_{xy} = \frac{\partial^2 g}{\partial x \partial y} \tag{3.6}$$

The Laplacian of g , is an estimation of the second order derivative along the gradient direction. In the context of edge detection, it is shown that the Laplacian is a good approximation to the second derivative along the gradient direction, providing that the curvature of the line of constant intensity that crosses the point under consideration is small. Moreover, the Laplacian is useless in the direction of junction edges.

$$\Delta^2 g = g_{xx} + g_{yy} \tag{3.7}$$

3.2.2 Discrete Differentiation

Digital images are sets of quantified samples corresponding to 2D array of pixels; then we need to represent them by discrete 2D function, and determine discrete approximations of the differential operators [39]-[40]. We define the intensity function of a digital image as mapping Z_RX $Z_C \rightarrow Z_I$ where Z_R, Z_C, and Z_I are a subset of Z=*{0, 1, 2, 3…}*, and present the row, column and intensity value of the pixels, respectively. The discrete function *g(r, c)* represents the color intensity of the pixel placed in row *r* and column *c*, and is an approximation obtained from sampling and quantization of analogue function *g(x, y)*. One of the simplest ways to approximate the first order derivatives g_x and g_y is through the calculation of the first differences along the main axes, i.e.:

$$g_c(c,r) = g(c,r) - g(c+1,r)$$
$$g_r(c,r) = g(c,r) - g(c,r+1) \tag{3.8}$$

3.2.3 Convolution

Convolution, in mathematics, is an operation on two functions producing third function that is typically viewed as a modified version of one of the original functions [39]. The discrete convolution of 2D function *f* and *g* is given by

$$(f * g) = \sum_{i=-\infty}^{\infty} \sum_{j=-\infty}^{\infty} f(i,j) g(r-i, c-j) \tag{3.9}$$

In image processing, the convolution is a general purpose filter that allows producing a range of effects by specifying a set of convolution kernels. It works by determining new value for a pixel by adding weighted values of all its neighboring pixels together. The applied weights are determined by a 2D array called convolution kernel or mask.

3.3 Conventional Operators

Nowadays, the images in the modern information society are becoming more and more prominent. Various image processing technologies are profoundly changing people's lives. Digital image processing as an important area of information technology, extensive attention has been unprecedented. Image processing problems due to the complexity and interdisciplinary nature of the problem for decades has been a research focus. Edge detection is an important part of digital image processing, which is the key step in image analysis, pattern recognition, and other deep-level processing. Integer-order edge detection is often used in image processing, especially first-order differential operation of the gradient operator and the second-order Laplacian, then find the local maximum (or crossing point).

3.3.1 First order Derivative filter

First order derivative edge gradient is obtained by forming running difference of pixels along rows and columns of the image [41]. The gradient of a function *f* (*x*, *y*) at coordinates (*x*, *y*) is defined as two dimensional column vector given as

$$\nabla \boldsymbol{f} \equiv \boldsymbol{grad}\left(\boldsymbol{f}\right) \equiv \begin{bmatrix} g_x \\ g_y \end{bmatrix} = \begin{bmatrix} \frac{\partial f}{\partial x} \\ \frac{\partial f}{\partial y} \end{bmatrix} \tag{3.10}$$

This vector points in the direction of the greatest rate of changes of *f*at location (*x*, *y*) . The magnitude (length) of vector ∇f denoted as *M*(*x*, *y*), where

$$M(x,y) = mag(\nabla f) = \sqrt{g_x^2 + g_y^2} \tag{3.11}$$

$M(x,y)$ is referred to as the gradient image. It has the same size as the original, created when x and *y* are allowed to vary over all pixel locations in *f*. Types of first order derivative filters are

$$\nabla \boldsymbol{f} \equiv \boldsymbol{grad}\left(\boldsymbol{f}\right) \equiv \begin{bmatrix} g_x \\ g_y \end{bmatrix} = \begin{bmatrix} \frac{\partial f}{\partial x} \\ \frac{\partial f}{\partial y} \end{bmatrix} \tag{3.12}$$

3.3.1.1 Sobel Operator

In a Sobel Operator slight variation from Prewitt operator in weight of central coefficient is done i.e. weight of 2 is used in center coefficient. The weight value of 2 is used to achieve some smoothing by giving more importance to central point [1]. The 3×3 Sobel mask used for x and y directions are [42].

$$\begin{bmatrix} -1 & -2 & -1 \\ 0 & 0 & 0 \\ 1 & 2 & 1 \end{bmatrix} \qquad \begin{bmatrix} -1 & 0 & 1 \\ -2 & 0 & 2 \\ -1 & 0 & 1 \end{bmatrix}$$

G_x G_y

Figure 3.2 Sobel Gradient in x and y Directions

It is seen that summation of all coefficients of the mask is zero hence in areas of constant gray level they give zero response. The effect of Sobel operator on an image is shown in Chapter 6.

3.3.1.2 Robert Cross Gradient Operator

It was one of the first edge detectors and was initially proposed by Lawrence Roberts in 1963 as a differential operator, the idea behind the Robert's Cross operator is to obtain Diagonal edge gradients by forming running differences of diagonal pairs of pixels [1]. The Roberts operator performs a simple, quick to compute, 2-D spatial gradient measurement on an image. It thus highlights regions of high spatial gradient which often correspond to edges. In its most common usage, the input to the operator is a gray scale image, as is the output. Pixel values at each point in the output represent the estimated absolute magnitude of the spatial gradient of the input image at that point. In theory, the operator consists of a pair of 2×2 convolution masks as shown [39]. One mask is simply the other rotated by 90°

$$\begin{bmatrix} 1 & 0 \\ 0 & -1 \end{bmatrix} \qquad \begin{bmatrix} 0 & 1 \\ -1 & 0 \end{bmatrix}$$

G_x G_y

Figure 3.3 Robert Gradient in x and y Directions

These masks are designed to respond maximally to edges running at 45° to the pixel grid, one mask for each of the two perpendicular orientations. The masks can be applied separately to the input image, to produce separate measurements of the gradient component in each orientation (call these G_x and G_y). These can then be combined together to find the absolute magnitude of the gradient at each point and the orientation of that gradient. The effect of applying Roberts Cross Gradient operator on an image is shown in Chapter 6.

3.3.1.3 Prewitt Operator

The Prewitt operator is used in image processing, particularly within edge detection algorithms [1]. Technically, it is a discrete differentiation operator, computing an approximation of the gradient of the image intensity function. At each point in the image, the result of the Prewitt operator is either the corresponding gradient vector or the norm of this vector. The operator calculates the gradient of the image intensity at each

point, giving the direction of the largest possible increase from light to dark and the rate of change in that direction. The result therefore shows how "abruptly" or "smoothly" the image changes at that point and therefore how likely it is that that part of the image represents an edge, as well as how that edge is likely to be oriented. The operator uses two 3 X 3 kernels which are convolved with the original image to calculate approximations of the derivatives one for horizontal changes, and one for vertical. The Prewitt 3 X 3 kernel used is given as [1]

$$\begin{bmatrix} -1 & -1 & -1 \\ 0 & 0 & 0 \\ 1 & 1 & 1 \end{bmatrix} \qquad \begin{bmatrix} -1 & 0 & 1 \\ -1 & 0 & 1 \\ -1 & 0 & 1 \end{bmatrix}$$

G_x G_y

Figure 3.4 Prewitt Gradient in x and y Directions

Applying the Prewitt operator on an image will provide an edge enhanced image as shown in Chapter 6. It is seen that contrast of edges enhanced is more than that by Roberts Operator.

3.3.2 Second order Derivative filter

Second order derivatives are employed when only edge magnitudes are of interest and without regard to their orientations. There are two types of operators which hold this kind of operators these are discussed below

3.3.2.1 Laplacian Filter

Laplacian have same properties in all directions and therefore is invariant to rotation in an image [1]. The Laplace operator is a very popular operator approximating the second derivative. The 3×3 masks for the four and eight neighborhoods used are:-

$$\begin{bmatrix} 0 & 1 & 0 \\ 1 & -4 & 1 \\ 0 & 1 & 0 \end{bmatrix} \qquad \begin{bmatrix} 1 & 1 & 1 \\ 1 & -8 & 1 \\ 1 & 1 & 1 \end{bmatrix}$$

G_X G_Y

Figure 3.5 Laplacian Gradient in x and y Directions

Effect of applying a Laplacian filter to the image is shown in Chapter 6.

3.3.2.2 Laplacian of Gaussian (LoG) Filter

In order to remove noise that occur in the Laplacian filtering, Laplacian of Gaussian filter is used. Marr-Hildreth have proposed the Laplacian of Gaussian Edge Detector [38]. Following steps are involved in LoG filtering.

- Smooth the image using Gaussian filter.
- .Enhance the edges using Laplacian operator.
- Zero crossings denote the edge locations.
- Use linear interpolation to determine sub-pixel location of edge.

It is defined as

$$LoG(x,y) = -\frac{1}{\pi\sigma^4}\left[1 - \frac{x^2+y^2}{2\sigma^2}\right]e^{-\frac{x^2+y^2}{2\sigma^2}} \qquad (3.13)$$

Greater the value of <broader is the Gaussian filter, more is the smoothing. But too much smoothing will make the detection of edges difficult. Figure 3.8 shows the effect of LoG filtering on an image

It can be observed that LoG filtering is less susceptible to noise unlike Laplacian so image sharpening is better using LoG filtering

Chapter 4

Fractional Differentiation

4.1 Introduction to Fractional Derivative

In the past few decades there has been raised concern about the fractional derivatives, especially due to its uses. A number of common problems regarding physics, geophysics, hydrology, economy etc. can be easily dealt by utilizing fractional calculus Fractional Differentiation is the branch of calculus that simplifies the derived value of a function to non-integer order, consenting the computations such as developing a function to 1/2 order. This part of integral differentiation is reflected as the unusual instance of fractional differentiation for while the fractional order value shifts to integer order values. The fractional derivative at a point *n* is a limited to fractional analysis only when fractional order is an integer; otherwise will not apply. Most definitions of fractional derivatives were known in the past. The most common one acquired through the integer order derivative has been discoursed here.

According to the general definition of integer order differentiation we can calculate the first order derivative of the signal x(t) as

$$x'(t) = \lim_{h\to 0} \frac{x(t) - x(t-h)}{h} \tag{4.1}$$

Similarly the second and third derivatives are given as

$$x''(t) = \lim_{h\to 0} \frac{x'(t) - x'(t-h)}{h} \tag{4.2}$$

$$x''(t) = \lim_{h\to 0} \frac{x(t) - 2x(t-h) + x(t-2h)}{h^2} \tag{4.3}$$

Delay operator is given as:

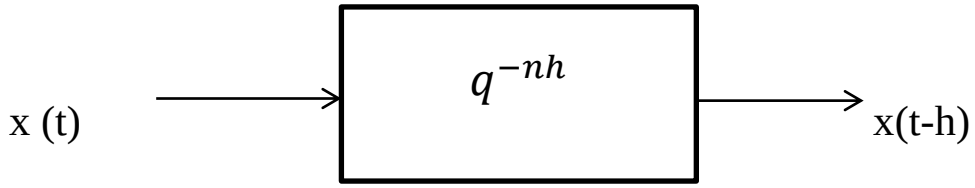

$$(1-q^{-h})^1 = 1-q^{-h} \tag{4.4}$$

$$(1-q^{-h})^2 = 1-2q^{-h}+q^{-2h} \tag{4.5}$$

$$(1-q^{-h})^m = \sum_{n=0}^{m}\binom{m}{n}\left(-q^{-h}\right)^n = \sum_{n=0}^{m}(-1)^n\binom{m}{n}q^{-nh} \tag{4.6}$$

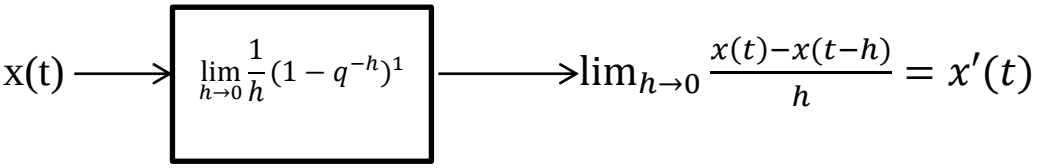

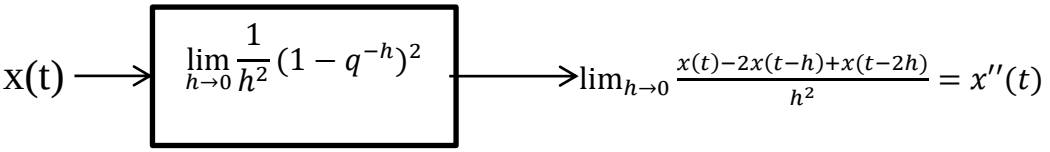

$$x^m(t) = \lim_{h\to 0}\frac{(1-q^{-h})^m}{h^m}x(t) \tag{4.7}$$

Replacing m by v from (4.7)

$$x^v(t) = \lim_{h\to 0}\frac{(1-q^{-h})^v}{h^v}x(t) \tag{4.8}$$

The fractional derivative of signal is given by using the equations (4.7) and (4.8).

$$x^v(t) = \lim_{h\to 0}\frac{1}{h^v}\left(\sum_{n=0}^{m}(-1)^n\binom{v}{n}q^{-nh}x(t)\right) \tag{4.9}$$

$$= \lim_{h\to 0}\sum_{n=0}^{m}h^{-v}(-1)^n\binom{v}{n}x(t-nh) \tag{4.10}$$

Equation (4.10) defines the G-L derivative. Assume that $v \in R$ where v is the integral part of R (real set), the signal $F(t) \in [a,t], a < t, a \in R, t \in R$, has m order continuous differentiation. m Is no less than $[v]$, when $v > 0$, then v-order differentiation could be expressed as [43].

$$D^{v}=\lim_{h\to 0}F^{(v)}(t)=\lim_{h\to 0}\frac{h^{(-v)}}{\Gamma(-v)}\sum_{m=0}^{n-1}(-1)^{m}\frac{\Gamma(m-v)}{\Gamma(m+1)}F(t-mh) \tag{4.11}$$

$\Gamma(x)=(x-1)!$ is gamma function of x.

$$D^{v}F(t)=D_{v}F(t)=\frac{d^{v}F(t)}{dt^{v}}\xleftrightarrow{FT}(\hat{D}_{v}F)(\omega)=(j\omega)^{v}.\hat{F}(\omega)=\hat{d}_{v}(\omega)\hat{F}(\omega) \tag{4.12}$$

where$v$order differential operator thatis $D_v = D$order differential multipliable operator of function $\widehat{d_v}(\omega) = (j\omega)^v$. The fractional differential filter function can be expressed as

$$\begin{cases}\hat{d}_{v}(\omega)=(j\omega)^{v}=\hat{a}_{v}(\omega).\exp(j\theta_{v}(\omega))=\hat{a}_{v}(\omega).p_{v}(\omega),\\ \hat{a}_{v}(\omega)=|\omega|^{v},\theta_{v}(\omega)=\frac{v\pi}{2}\operatorname{sgn}(\omega)\end{cases} \tag{4.13}$$

4.2 Characteristics of Fractional Derivative

The concept of derivative is usually associated to an integer; as a function which can be derived by one, two, three times and so on. The main approach is to examine the properties of ordinary derivative and examine how and where it is possible to derive the concepts. Here we use the most intuitive and less rigorous way to generalize the concept. Take a derivative S and consider its general properties that are applicable to fractional derivative. Fractional derivative has the following properties:

(1) Associative Law: According to this property for a function $f(t)$ and constant C.

$$D_{t}^{v}\left[Cf(t)\right]=CD_{t}^{v}\left[f(t)\right] \tag{4.14}$$

(2)Distributive Law: For the function $f(t)$ and $g(t)$

$$D_{t}^{v}\left[f(t)\pm g(t)\right]=D_{t}^{v}\left[f(t)\right]\pm D_{t}^{v}\left[g(t)\right] \tag{4.15}$$

(3)The operator obeys Leibniz rule by taking the derivative of product of two functions

$$D_{t}^{v}\left[f(t)g(t)\right]=\sum_{n=0}^{v}D_{t}^{v-n}\left[f(t)\right]D_{t}^{n}\left[g(t)\right] \tag{4.16}$$

4.3 Physical Meaning of Fractional Derivative

The physical meaning of a signal's fractional differential is defines in equation number (4.12) that established amplitude-and-phase modulation from estimation of information theory that point outs that it is fractional phase and frequency-modulation [43]. From the results it is conclude that amplitude of original signal is changing with its frequency as fractional power exponent while phase is derived Hilbert transform of frequency.

The v order can be expressed as follows by using equation (4.11):

$$\Delta^{v}F = \frac{1}{\Gamma(-v)}\sum_{m=0}^{n}\frac{\Gamma(m-v)}{\Gamma(m+1)}F(t-mh) \tag{4.17}$$

So v is a generalized or common difference. Put the integral differential expression into equation (4.14), where integral difference is a special example of fractional difference. The fractional slope can be defined as a generalized function curve of fractional derivative. Fractional integral is generally the Euclidean measurement for normal geometric image that is called Fractional Euclidean measurement [44]. From kinetic perspective, fractional derivative is generalized derivative and the mathematic generalization for generalized speed and flow. Thus, it can be analyze that the physical meaning of fractional derivative is fractional speed and fractional flow. Generalized acceleration introduces generalized speed.

When order is in [0, 1] i.e. low order, fractional speed is generalized speed; it is the continuous interpolation of fractional time between first order speed vector and zero order displacement vector. When the order is in [0, 1], it has low order measurements for temporal balance state. It has the fractional time continuous interpolation between first order speed and zero order displacement proven by low order speed. The difference is not absolute between them. It has two movement models of physical movement being discrete, continuous and one universal model being discrete and continuous. Gradient vector is the change from linear time-space view to curve time-space view. It does not always orientate the maximum descending way. First order fractional speed is generalized the fractional time continuous interpolation and acceleration between m and m+1 acceleration vector. It is the high order measurement when order is > 1 for temporal balance state and fractional continuous measurement for speed change. Thus, it is said

that traditional acceleration and speed is the special case for fractional speed and acceleration.

Take $\phi(t)$ (Gauss signal) in figure 4.1 [33] discuss the numerical implement of any order derivative. ν=0.00 means original signal is not differential or integral. The limit of the fractional differential operator is $\left|D^{\nu}s(t)\right| = \left|s^{\nu}(t)\right| < \infty$. It is continuous, i.e. $\lim_{1\to 2} D^{\nu 1}s(t) = D^{\nu 2}s(t)$ where $\nu 1, \nu 2 \in R$. In other terms, fractional differential is the continuous interpolation of neighborhood order. Here $D^{\nu}s(t)$ is the real number. $D^{\nu}[0] = 0$ for any ν order fractional differential. Here [0] shows unit leaping signal whose amplitude is always zero. Fractional differential is non-zero for non-zero amplitude of unit leaping signal. $\varphi^{\nu}(t)$ represents fractional gradient vector. It orientates the maximum descending direction when ν is integer. $\varphi^{\nu}(t)$ represents the fractional measurement of points in curve $\varphi^{\nu}(t)$. $\varphi^{1}(t) = 0$ in temporal equilibrium is stationary point of curve $\varphi^{\nu}(t)$ and the first order temporal equilibrium point, which may be a stable equilibrium point or an unstable one. It is observed that the first order derivative is the measurement for temporal equilibrium state not for temporal stable state. The temporal stable state of the point of the curve depends on the co-effect of the characteristic of concavity & convexity and on the concavity or convexity of the curve or curve surface and temporal balance state. In other terms the generalized stationary point corresponding to $\varphi^{\nu}(t)$=0 is ν order temporal fractional balanced point.

From Figure 4.1, it is seen that the first order stationary point has non-zero fractional differentiation. Generally, first order stationary points and fractional stationary points are non-identity. Similarly, the fractional differential of first order stationary point is non-zero while its first order differential in two dimensional curve surfaces is zero. So if time t changes as $-\infty \to 0 \to \infty$, the order ν of $\varphi^{\nu}(t) = 0$ varies as $0 \to 1 \to \infty$, fractional differential is continuous. When order is between (1, ∞), fractional derivative indicates the high order and fractional stationary point of signal on the ascending section of signal

$\varphi(t)$ when $t \in (-\infty, 0)$. When order is between [0, 1]) on descending section while $t \in (0, \infty)$.

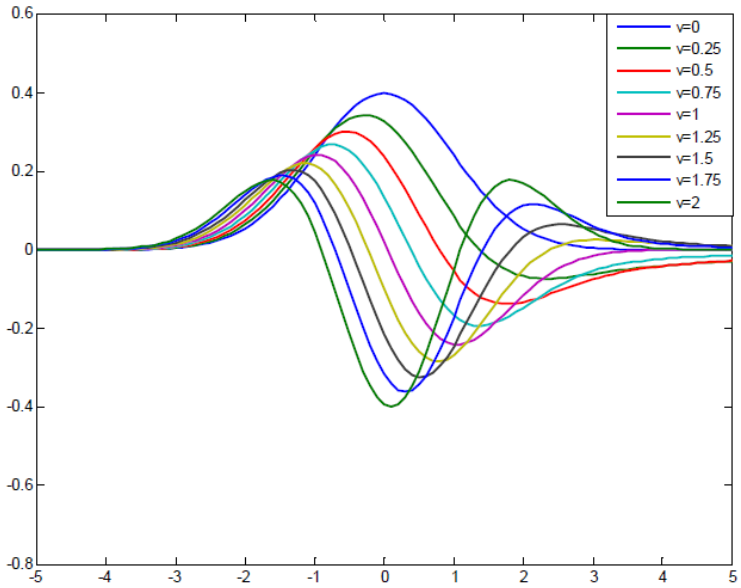

Figure 4.1 Different fractional order fractional differential of normal Gaussian signal [33]

The even symmetric signal has fractional derivative not symmetric and cannot keep its symmetry unchanged before and after fractional differential. The higher order stationary points have fractional differential that are non-symmetrical. In other words, the even points on even symmetric curve have not same temporal balance state that keep changing with integral differential. At the same the lower fractional derivative has single apex curve, abrupt descending, and with long negative tail. It crosses zero line for only one time and has only one lower order (when order is between [0, 1]) stationary point. The lower fractional derivative curve, the higher one and the zero line of vertical axis may intersect at the same point. The lower fractional derivative curve, the higher one and the zero line of vertical axis may intersect at the same point. The stationary point of the higher order (when order is >1) and the lower order (when order is between [0, 1]) may be the same point. The fractional order v is fractional description for temporal balance state, and it is called fractional equilibrium coefficient [33].

4.4 Fractional Differential Detection for Image Texture Detail Feature

The filter function of fractional differential filter is $d_v(w) = (jw)^v = |w|^v = \exp(j\theta_v(w))$ Amplitude characteristic is even function and phase characteristic is odd function. Analyzing the characteristics of fractional differential filter for $w > 0$, the frequency response of fractional differential filter is given in Figure 4.2.It is observed that, in viewpoints of signal processing, the frequency response of fractional differential is actually a nonlinear filter when v=0, v-order fractional differential is all-pass filter, and its frequency response is $d_v(w)$=0=> $d_v(t) = \delta(t)$ [37].when v<0 it is a fractional integrator and is singular low-pass integral filter. When v>0 it is fractional derivative operator. Its frequency response is $\lim_{|w\to\infty|} |d_v(w)| = \infty$. Here $|d_v(w)|$ is singular high pass differential filter. as v is increasing, high pass characteristics becomes stronger and transmission band of $|d_v(w)|$ become narrower.

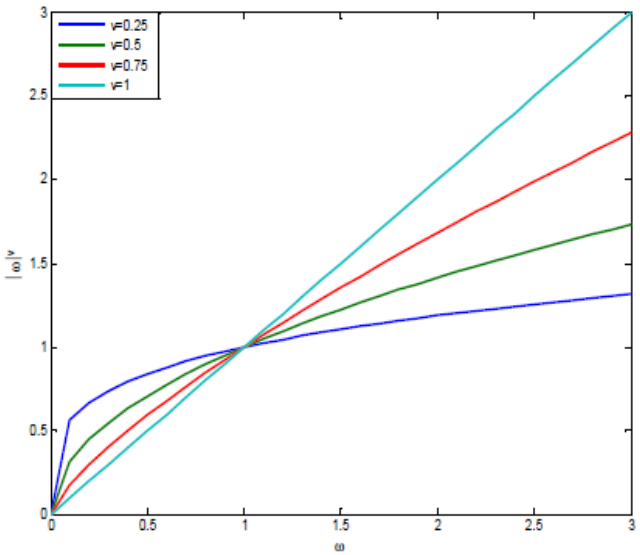

Figure 4.2 Frequency response of Fractional Differential operator [45]

In other words as v increases, it non-linearly enhances its high frequency components and nonlinearly inhibits its low frequency components. When $0 < v < 1$ the enhancement of high-frequency components by fractional differential is less than integral one, and the enhancement of high frequency edge components by fractional differential is

inferior to that of first-order one. The preservation magnitude of low frequency contour by fractional differential is superior to that by first-order one for extremely low frequency components ($0 < w < 1$).first-order differential is linear one while fractional differential is a nonlinear attenuator. The attenuation of low frequency components is less when v is smaller. It behaves like all pass filter when $v \to 0$. The texture features in smooth area may be greatly attenuating and its differential result is nearly zero (the integral differential of constant is zero) at Image's smooth area whose gray scale is constant. It occurs when image is filtered by first order differential based operator such as Prewitt operator, or by second order based operator such as Laplacian operator [45]. Due to this reason integral differential linearly attenuates texture features and could not hold them in smooth areas.

On the other hand fractional differential operator preserve textural feature in smooth areas in large scale. Fractional differential-based operator is superior to integral differential-based in enhancing the texture in smooth area. The characteristic of fractional differential and fractional differential mask is analyzed by doing fractional differential for rectangle wave signal and saw-tooth wave signal. The results are shown in Figure 4.3

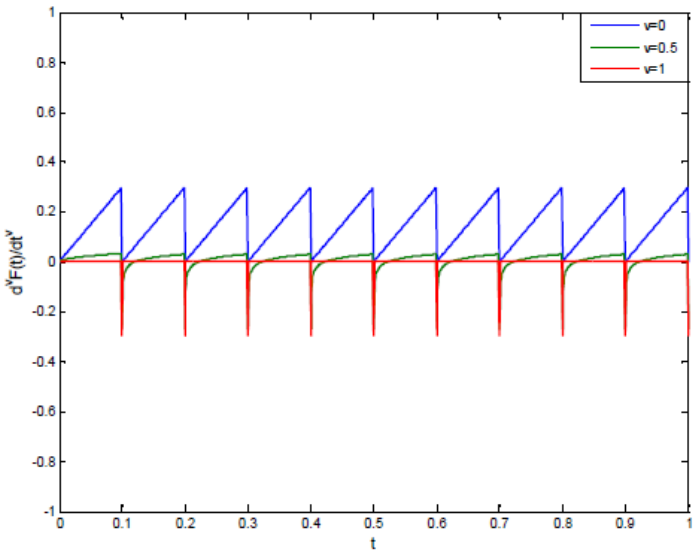

(a)

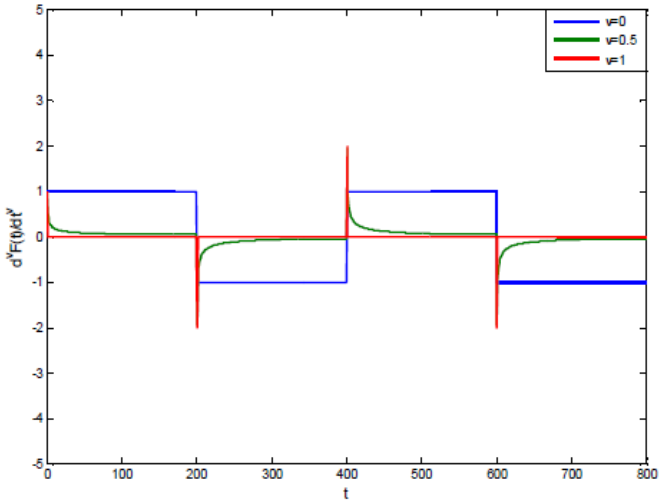

(b)

Figure 4.3 Characteristics Analyzing for Fractional Differential (a) First order and fractional differential of a Rectangular Wave (b) First order and fractional differential of a Saw tooth Wave [45]

In the Figure 4.3(a), fractional differential in smooth area is from the biggest value in the singular leaping point to zero which is the remarkable difference between fractional integral operator and fractional differential. There is non-linearly enhance of high frequency singular information. When v=1, integral differential of high-frequency singular signal is Dirac signal. The enhancement of high-frequency singular is small at $0 < v < 1$ than at v=1. Thus integral differential is the special case of fractional differential. In the Figure 4.5(b), the fractional differential of the slope is non-linear curve, not zero or constant.

From the discussion, it can be examine that fractional differential could non-linearly enhance high-frequency marginal information in those areas where gray scale changes frequently, and nonlinearly enhance texture details in those areas where gray scale is constant as well as could nonlinearly preserve the low-frequency contour feature in the smooth area .

Chapter 5

Fractional Order Differential Operator

Fractional differential is more efficient in edge detection than the integral differential techniques that it not only preserves the low frequency components but also enhance the high frequency components of image [35]. There are number of fractional differential equations are available but the most common used are Grumwald-Letnikov and Riemann-Liouville equations. Fractional differential mask or filters are designed by using these equations and are applied on images for edge detection. An improved G-L fractional differential filer is discussed as:

5.1 An Improved Grumwald-Letnikov Fractional Differential Filter

Fractional differential filter can be construed from the integer-order differentiation filter [41-43]. Fractional differential finite impulse (FIR) filters transfer function as follows:

$$D^{v}(z)=\left(\frac{1-z^{-1}}{T}\right)^{v} \tag{5.1}$$

By the reference of binomial series expansion $(1+y)^{v}=1+vy+\sum_{k=2}^{\infty}\frac{v(v-1)....(v-k+1)}{k!}y^{k}$, and replace $-z^{-1}$ instead of y, the above equation can be written as:

$$D^{v}(z)=\frac{1}{T^{v}}\left(1-vz^{-1}+\sum_{i=2}^{\infty}\frac{v(v-1)....(v-i+1)}{i!}\left(-z^{-1}\right)^{-i}\right) \tag{5.2}$$

$$=\frac{1}{T}\sum_{i=0}^{\infty}(-1)^{i}\frac{\Gamma(v+1)}{\Gamma(i+1)\Gamma(v-i+1)} \tag{5.3}$$

Here z is the displacement factor; T is the sampling period and $\Gamma(.)$ is gamma function.

5.1.1 Design of an Improved Grumwald-Letlinkov Fractional Differential Operator

Select the suitable N according to the limited impact of fractional differential filter transfer function, from which the given formula is obtained.

$$D^{v}(z)=\left(\frac{1-z^{-1}}{T}\right)\approx\frac{1}{T^{v}}\sum_{i=0}^{N}(-1)^{i}\frac{\Gamma(v+1)}{\Gamma(i+1)\Gamma(v-i+1)}z^{-i} \tag{5.4}$$

From above it can get signal differential equation:

$$\frac{d^{v}f(t)}{dt^{v}}\approx f(t)+(-v)f(t-1)+\frac{v(v-1)}{2}f(t-2)+.....+(-1)^{n}\frac{\Gamma(v+1)}{n!\Gamma(v-n+1)}f(t-n) \tag{5.5}$$

For digital images, based on the signal difference equation, fractional differential gradient formula can be obtained in different directions.

Vertical direction

$$D^{v}_{YU\leftrightarrow YD}=a_1I(x,y-1)-a_1I(x,y+1)+.....+a_nI(x,y-n)-a_nI(x,y+n) \tag{5.6}$$

Horizontal direction

$$D^{v}_{XL\leftrightarrow XR}=a_1I(x-1,y)-a_1I(x+1,y)+.....+a_nI(x-n,y)-a_nI(x+n,y) \tag{5.7}$$

135^{o} Direction

$$D^{v}_{LU\leftrightarrow RD}=a_1I(x-1,y-1)-a_1I(x+1,y+1)+.....+a_nI(x-n,y-n)-a_nI(x+n,y+n) \tag{5.8}$$

45^{O} Direction

$$D^{v}_{RU\leftrightarrow LD}=a_1I(x+1,y-1)-a_1I(x-1,y+1)+.....+a_nI(x+n,y-n)-a_nI(x-n,y+n) \tag{5.9}$$

Here, $a_1 = -v$, $a_2 = \frac{v(v-1)}{2}$, $a_3 = \frac{-v(v-1)(v-2)}{6}$, $a_4 = \frac{v(v-1)(v-2)(v-3)}{24}$,……,

$$a_n = (-1)^n \frac{\Gamma(v+1)}{n!\Gamma(v-n+1)} \tag{5.10}$$

By using these equations, construct 5×5 fractional order differential operator.

0	0	0	0	0
0	0	0	0	0
$\frac{(v^2-v)}{2}$	-v	0	v	$\frac{(v-v^2)}{2}$
0	0	0	0	0
0	0	0	0	0

Figure 5.1.Horizontal left-right direction

0	0	$\frac{(v^2-v)}{2}$	0	0
0	0	-v	0	0
0	0	0	0	0
0	0	v	0	0
0	0	$-\frac{(v^2-v)}{2}$	0	0

Figure 5.2. Vertical up-down direction

$\frac{(v^2-v)}{2}$	0	0	0	0

0	-v	0	0	0
0	0	0	0	0
0	0	0	v	0
0	0	0	0	$-\frac{(v^2-v)}{2}$

Figure 5.3.135 Degree left-up to right-down direction

0	0	0	0	$\frac{(v^2-v)}{2}$
0	0	0	-v	0
0	0	0	0	0
0	v	0	0	0
$-\frac{(v^2-v)}{2}$	0	0	0	0

Figure 5.4. 45 Degree right-left direction

0	0	0	0	0
0	0	0	0	0
$\frac{(v-v^2)}{2}$	v	0	-v	$\frac{(v^2-v)}{2}$
0	0	0	0	0
0	0	0	0	0

Figure 5.5. Horizontal right-left direction

0	0	$-\frac{(v^2-v)}{2}$	0	0
0	0	v	0	0
0	0	0	0	0
0	0	-v	0	0
0	0	$\frac{(v^2-v)}{2}$	0	0

Figure 5.6. Vertical down-up direction

$-\frac{(v^2-v)}{2}$	0	0	0	0
0	v	0	0	0
0	0	0	0	0
0	0	0	-v	0
0	0	0	0	$\frac{(v^2-v)}{2}$

Figure 5.7. 135 Degree left-up to right-down direction

0	0	0	0	$-\frac{(v^2-v)}{2}$
0	0	0	V	0
0	0	0	0	0
0	-v	0	0	0
$\frac{(v^2-v)}{2}$	0	0	0	0

Figure 5.8. 45 Degree left-right direction

5.1.2 Combination of Robert and Fractional Order Differential Mask

In digital image f(x, y), the gradient at point f(x, y) can be expressed as:

$$\nabla f(x,y) = \left[G_x \;\; G_y \right]^T \tag{5.11}$$

$$= \left[\frac{\partial f}{\partial x} \;\; \frac{\partial f}{\partial y} \right]^T \tag{5.12}$$

The difference of mutually perpendicular directions can be considered as the gradient approximation. Robert proposed the following equation :

$$g(x,y) = \left| \nabla f(x,y) \right| = \left\{ \left[f(x,y+1) - f(x+1,y) \right]^2 + \left[f(x+1,y+1) - f(x,y) \right]^2 \right\}^{1/2} \tag{5.13}$$

Edge detection with Robert operator is performed by convolving the original image with the following masks:

1	0
0	-1

0	1
-1	0

Figure 5.9 Robert Mask on two orientations (a) G_x (b) G_y

The fractional order G-L definition can be expressed as [4][v] Is the integral part when $s(t) \in [a,t](a < t, a \in R, t \in R)$. It has m+1 order continuous derivative. Minimum m is [v] when v>0.

$$\text{When } \begin{bmatrix} -v \\ r \end{bmatrix} = \frac{(-v)(-v+1)....(-v+r-1)}{r!} \tag{5.14}$$

When $n \to \infty, h \to 0, S_n^{(-v)}(t)$ meets to non-zero limit.

$$n = \left[\frac{t-a}{h} \right] \text{ When } h = \frac{t-a}{n} \tag{5.15}$$

From equation (5.5), suppose the duration of monadic signal f(t) is $t \in [a,t]$ and then averagely divide the signal duration. If it has $n = \left[\frac{t-a}{h} \right] = [t-a]$ when h=1. The differentiation of monadic signal $f(t)$ can be expressed as [7-10].

$$\frac{d^v f(t)}{dt^v} \approx f(t) + (-v) f(t-1) + \frac{(-v)(-v+1)}{2!} f(t-2) + ... + \frac{\Gamma(-v+1)}{n!\Gamma(-v+n+1)} f(t-n) \tag{5.16}$$

The fractional partial differential of backward difference on negative x and y coordinate for two dimensional image f(x, y) can be expressed as:

$$\frac{d^{v} f(x,y)}{dx^{v}} \approx f(x,y) + (-v) f(x-1,y) + \frac{(-v)(-v+1)}{2!} f(x-2,y) + \ldots + \frac{\Gamma(-v+1)}{n!\Gamma(-v+n+1)} f(x-n,y) \tag{5.17}$$

$$\frac{d^{v} f(x,y)}{dx^{v}} \approx f(x,y) + (-v) f(x,y-1) + \frac{(-v)(-v+1)}{2!} f(x,y-2) + \ldots + \frac{\Gamma(-v+1)}{n!\Gamma(-v+n+1)} f(x,y-n) \tag{5.18}$$

The distinct difference between fractional differential based processing and an integral one is the summation of all non-zero coefficients which is not zero. From equations (5.17) and (5.18), we can form the fractional differential mask of 3*3 on eight central symmetric directions, which are positive x and y coordinate, negative x and y coordinate, right upward diagonal, left downward diagonal, left upward diagonal and right downward diagonal.

0	$\frac{v^2 - v}{2}$	0
0	-v	0
0	1	0

(a)

0	0	0
$\frac{v^2 - v}{2}$	-v	1
0	0	0

(b)

$\frac{v^2 - v}{2}$	0	0
0	-*v*	0
0	0	1

(c)

0	0	$\frac{v^2 - v}{2}$
0	-*v*	0
1	0	0

(d)

Figure 5.10 Fractional differential mask on eight orientations. (a) negative*x* -coordinate. (b) positive*y* -coordinate.(c)right downward diagonal. (d)left upward diagonal.

Robert uses difference of two diagonal adjacent pixels to detect gradient magnitude. Because of edge detection of smaller number of pixels and position accuracy, edge lines are not sharp enough and are smaller. These edges are sensitive to noise. If fractional order differential operator is combined with the Robert operator it enhances the image texture and recognizes the edges of small and prominent.The combination formula is given as:

$$D^v[g(x,y)] = \frac{\partial^v g(x,y)}{\partial x^v} + \frac{\partial^v g(x,y)}{\partial y^v} \tag{5.19}$$

$$\frac{\partial^{v} g(x,y)}{\partial x^{v}} \approx g(x,y) + (-v)g(x-1,y) + \frac{(-v)(-v+1)}{2} g(x-2,y) + \ldots. + \frac{\Gamma(-v+1)}{n!\Gamma(-v+n+1)} g(x-n,y) \tag{5.20}$$

By adding the equation number (5.20) with equation (5.13), we get the results as:

$$= \left\{ \left[f(x,y+1) - f(x+1,y) \right]^2 + \left[f(x+1,y+1) - f(x,y) \right]^2 \right\}^{1/2} +$$

$$(-v) \left\{ \left[f(x-1,y+1) - f(x,y) \right]^2 + \left[f(x,y+1) - f(x-1,y) \right]^2 \right\}^{1/2} +$$

$$\frac{(-v)(-v+1)}{2} \left\{ \left[f(x-2,y+1) - f(x-1,y) \right]^2 + \left[f(x-1,y+1) - f(x-2,y) \right]^2 \right\}^{1/2} + \ldots\ldots. +$$

$$\frac{\Gamma(-v+1)}{n!\Gamma(-v+n+1)} \left\{ \left[f(x-n,y+1) - f(x-n+1,y) \right]^2 + \left[f(x-n+1,y+1) - f(x-n,y) \right]^2 \right\}^{1/2} \tag{5.21}$$

$$\frac{\partial^{v} g(x,y)}{\partial y^{v}} \approx g(x,y) + (-v)g(x,y-1) + \frac{(-v)(-v+1)}{2} g(x,y-2) + \ldots + \frac{\Gamma(-v+1)}{n!(-v+n+1)} g(x,y-n) \tag{5.22}$$

Now combine the equation (5.13) with equation (5.22) then get the result as:

$$= \left\{ \left[f(x,y+1) - f(x+1,y) \right]^2 + \left[f(x+1,y+1) - f(x,y) \right]^2 \right\}^{1/2} +$$

$$(-v) \left\{ \left[f(x,y) - f(x+1,y-1) \right]^2 + \left[f(x+1,y) - f(x,y-1) \right]^2 \right\}^{1/2} +$$

$$\frac{(-v)(-v+1)}{2} \left\{ \left[f(x,y-1) - f(x+1,y-2) \right]^2 + \left[f(x+1,y-1) - f(x,y-2) \right]^2 \right\}^{1/2} + \ldots\ldots +$$

$$\frac{\Gamma(-v+1)}{n!\Gamma(-v+n+1)} \left\{ \left[f(x,y-n+1) - f(x+1,y-n) \right]^2 + \left[f(x+1,y-n+1) - f(x,y-n) \right]^2 \right\}^{1/2} \tag{5.23}$$

5.1.3 Combination of Sobel and Fractional Order Differential Mask

Edges are the points where the discontinuity in intensity function or sharp intensity gradient in the image. The gradient of an image can be defined as:

$$\nabla f(x,y) = \left[G_x \; G_y \right]^T \tag{5.24}$$

$$G_x = f(x+1,y) - f(x,y) \tag{5.25}$$

$$G_y = f(x,y+1) - f(x,y) \tag{5.26}$$

Sobel is a classical first order derivative detection method that detects horizontal and vertical edges of image. Sobel mask of 3*3 is given as:

-1	-2	-1
0	0	0
1	2	1

(a)

-1	0	1
-2	0	2
-1	0	1

(b)

Figure 5.11 Sobel mask (a) G_X(b) G_Y

Mask can be applied separately to 3*3 neighborhoods of pixels that are at center. The gradient of image can be found using the following approximations:

$$G_x = -f(x-1,y-1) + f(x+1,y-1) - 2f(x-1,y) + 2f(x+1,y) - f(x-1,y+1) + f(x+1,y+1) \tag{5.27}$$

$$G_y = -f(x-1,y-1) + f(x-1,y+1) - 2f(x,y-1) + 2f(x,y+1) - f(x+1,y-1) + f(x+1,y+1) \tag{5.28}$$

The differential form of the gradient component can be given by the below approximations as:

$$G_x = \frac{1}{2}\left(\frac{\partial f(x+1,y-1)}{\partial x} + 2\frac{\partial f(x+1,y)}{\partial x} + \frac{\partial f(x+1,y+1)}{\partial x} \right) \tag{5.29}$$

$$G_y = \frac{1}{2}\left(\frac{\partial f(x-1, y+1)}{\partial y} + 2\frac{\partial f(x, y+1)}{\partial y} + \frac{\partial f(x+1, y+1)}{\partial y} \right) \tag{5.30}$$

In various scientific fields including image processing fractional order derivative is used [7-9]. Suppose the size of image is $M \times N$, by using Grunwald-Letnikov definition [10], the discrete form of $\nabla^v f$ can be represented as:

$$(\nabla^v f)_{i,j} = ((\Delta_1^v f)_{i,j}, (\Delta_2^v f)_{i,j}) \qquad 1 \le i < M, 1 \le j \le N \tag{5.31}$$

With

$$\left(\nabla_1^v f\right)_{i,j} = \sum_{n=0}^{N} (-1)^n C_n^v f_{i-n,j} \tag{5.32}$$

$$\left(\nabla_2^v f\right)_{i,j} = \sum_{n=0}^{N} (-1)^n C_n^v f_{i-n,j} \tag{5.33}$$

where N ≥ 3 is an integer constant and $C_n^v = \dfrac{\Gamma(v+1)}{\Gamma(n+1)\Gamma(v-n+1)}$ where Γ is the gamma function.

From equation (5.29) and (5.30), differential form of fractional-order gradient can be formed as:

$$G^v{}_x = \frac{1}{2}\left(\frac{\partial^v f(x+1, y-1)}{\partial x^v} + 2\frac{\partial^v f(x+1, y)}{\partial x^v} + \frac{\partial^v f(x+1, y+1)}{\partial x^v} \right) \tag{5.34}$$

$$G^v{}_y = \frac{1}{2}\left(\frac{\partial^v f(x-1, y+1)}{\partial y^v} + 2\frac{\partial^v f(x, y+1)}{\partial y^v} + \frac{\partial^v f(x+1, y+1)}{\partial y^v} \right) \tag{5.35}$$

By using the given calculations, the fractional order gradient component along the x and y directions can be found as:

$$G_x^v = \frac{1}{2}\begin{bmatrix} f(x+1, y-1) - vf(x, y-1) + \dfrac{v^2 - v}{2} f(x-1, y-1) + \ldots \\ +(-1)^n C_n^v f(x+1-n, y-1) + 2f(x+1, y) - 2vf(x, y) + (v^2 - v) f(x-1, y) \\ +\ldots + 2*(-1)^n C_n^v f(x+1-n, y) + f(x+1, y+1) - vf(x, y+1) + \dfrac{v^2 - v}{2} f(x-1, y+1) + \ldots + \\ (-1)^n C_n^v f(x+1-k, y+1) \end{bmatrix} \tag{5.36}$$

$$G_y^v = \frac{1}{2}\begin{bmatrix} f(x-1,y+1) - vf(x-1,y) + \frac{v^2-v}{2} f(x-1,y-1) \\ +\ldots+(-1)^n C_n^v f(x-1,y+1-k) + f(x,y+1) - vf(x,y) + (v^2-v) f(x,y-1) \\ +\ldots+(-1)^n C_n^v f(x,y+1-n) + f(x+1,y+1) - \\ vf(x+1,y) + \frac{v^2-v}{2} f(x+1,y-1) + \ldots + (-1)^n C_n^v f(x+1,y+1-n) \end{bmatrix} \quad (5.37)$$

$\frac{(-1)^n C_n^v}{2}$	:	$\frac{-v^2-v}{4}$	$\frac{-v}{2}$	$\frac{1}{2}$
$(-1)^n C_n^v$	:	$\frac{-v^2-v}{2}$	$-v$	1
$\frac{(-1)^n C_n^v}{2}$	:	$\frac{-v^2-v}{4}$	$\frac{-v}{2}$	$\frac{1}{2}$

(a)

$\frac{(-1)^n C_n^v}{2}$	$(-1)^n C_n^v$	$\frac{(-1)^n C_n^v}{2}$
:	:	:
$\frac{v^2-v}{4}$	$\frac{v^2-v}{2}$	$\frac{v^2-v}{2}$
$\frac{-v}{2}$	$-v$	$\frac{-v}{2}$

(b)

Figure 5.12 Fractional Order Sobel mask

The fractional derivative involves infinite number of terms while integer derivative contains finite terms. Hence, fractional mask contains more information than integer order derivative. Fractional derivative is global operator while integer order is a local operator.

5.1.4. Combination of Pewitt and Fractional Order Differential Mask

Prewitt is a classical first order derivative detection method that detects horizontal and vertical edges of image. It is different from Sobel operator by weight. Mask of 3*3 is given as:

-1	-1	-1
0	0	0
1	1	1

Figure 5.13 Prewitt Horizontal Mask

-1	0	1
-1	0	1
-1	0	1

Figure 5.14 Prewitt Vertical Mask

This mask is applied to the image and it detects the horizontal and vertical edges. The gradient of image is given by using the following calculation:

$$G_x = -f(x-1,y-1) + f(x+1,y-1) - f(x-1,y) + f(x+1,y) - f(x-1,y+1) + f(x+1,y+1) \quad (5.38)$$

$$G_y = -f(x-1,y-1) + f(x-1,y+1) - f(x,y-1) + f(x,y+1) - f(x+1,y-1) + f(x+1,y+1) \quad (5.39)$$

Gradient component can be found using given approximations:

$$G_x = \frac{1}{2}\left(\frac{\partial f(x+1,y-1)}{\partial x} + \frac{\partial f(x+1,y)}{\partial x} + \frac{\partial f(x+1,y+1)}{\partial x} \right) \quad (5.40)$$

$$G_y = \frac{1}{2}\left(\frac{\partial f(x-1,y+1)}{\partial y} + \frac{\partial f(x,y+1)}{\partial y} + \frac{\partial f(x+1,y+1)}{\partial y} \right) \quad (5.41)$$

By using Grunwald-Letnikov definition, where $C_n^v = \frac{\Gamma(v+1)}{\Gamma(n+1)\Gamma(v-n+1)}$ .Differential form of Fractional order differential gradient can be given as using (5.40) and (5.41) given approximations:

$$G^v{}_x = \frac{1}{2}\left(\frac{\partial^v f(x+1,y-1)}{\partial x^v} + \frac{\partial^v f(x+1,y)}{\partial x^v} + \frac{\partial^v f(x+1,y+1)}{\partial x^v} \right) \tag{5.42}$$

$$G^v{}_y = \frac{1}{2}\left(\frac{\partial^v f(x-1,y+1)}{\partial y^v} + 2\frac{\partial^v f(x,y+1)}{\partial y^v} + \frac{\partial^v f(x+1,y+1)}{\partial y^v} \right) \tag{5.43}$$

The fractional order gradient component along x and y direction can be found by using the following calculations:

$$G_x^v = \frac{1}{2}\begin{bmatrix} f(x+1,y-1) - vf(x,y-1) + \frac{v^2-v}{2} f(x-1,y-1) + \dots \\ +(-1)^n C_n^v f(x+1-n,y-1) + f(x+1,y) - vf(x,y) + (v^2-v) f(x-1,y) \\ +\dots+(-1)^n C_n^v f(x+1-n,y) + \\ f(x+1,y+1) - vf(x,y+1) + \frac{v^2-v}{2} f(x-1,y+1) + \dots + \\ (-1)^n C_n^v f(x+1-k,y+1) \end{bmatrix} \tag{5.46}$$

$$G_y^v = \frac{1}{2}\begin{bmatrix} f(x-1,y+1) - vf(x-1,y) + \frac{v^2-v}{2} f(x-1,y-1) \\ +\dots+(-1)^n C_n^v f(x-1,y+1-k) + \\ f(x,y+1) - vf(x,y) + (v^2-v) f(x,y-1) \\ +\dots+(-1)^n C_n^v f(x,y+1-n) + f(x+1,y+1) - vf(x+1,y) + \frac{v^2-v}{2} f(x+1,y-1) \\ +\dots+(-1)^n C_n^v f(x+1,y+1-n) \end{bmatrix} \tag{5.47}$$

Chapter 6
Results and Discussions

The edge detection and noise reduction capability of an improved fractional differential is analyzed by qualitatively comparing it with other types edge detection techniques. While the edge detection of an image using any edge detection technique, the information in the resultant image might be decreased or increased.

6.1 Edge Detection Analysis

Edge detection process is conducted on noiseless Lena image. First we apply Sobel operator, second Prewitt operator, third Robert operator, for Laplacian operator, fifth fractional operator. After that same edge detection operators are applied on the noisy Lena image.

6.1.1 Edge Detection by using Sobel Operator on noiseless and noisy Lena Image

The results for the image of lena used with the operator Sobel with a noise-free environment and with Gaussian and Salt & pepper noise are discussed below.

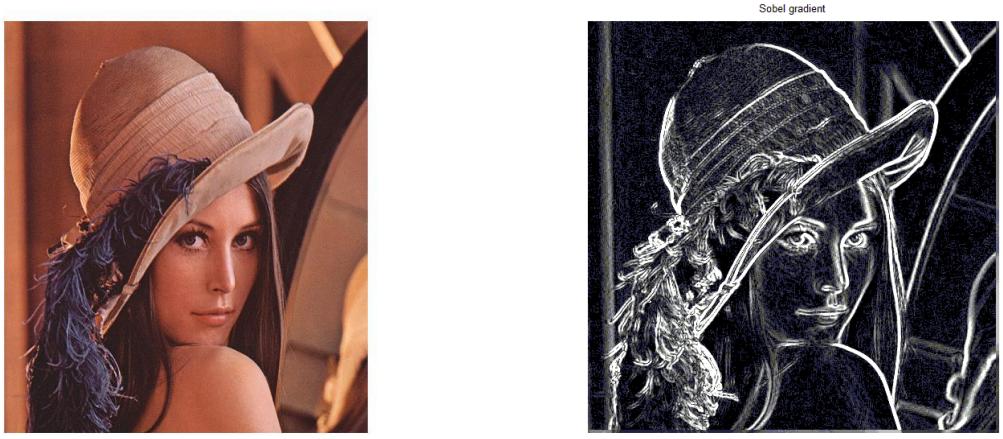

(a) **(b)**

Figure 6.1. (a) original lena image **(b)** Edge detection of noiseless Lena Image using Sobel Operator.

(a) (b)

Figure 6.2. (a) Lena image with Gaussian noise (b) Edge detection of Lena Image with Gaussian Noise using Sobel Operator.

(a) (b)

Figure 6.3. (a) Lena image with Salt & Pepper noise (b) Edge detection of Lena Image with Salt & Pepper Noise using Sobel Operator.

6.1.2. Edge Detection by using Prewitt Operator on noiseless and noisy Lena Image

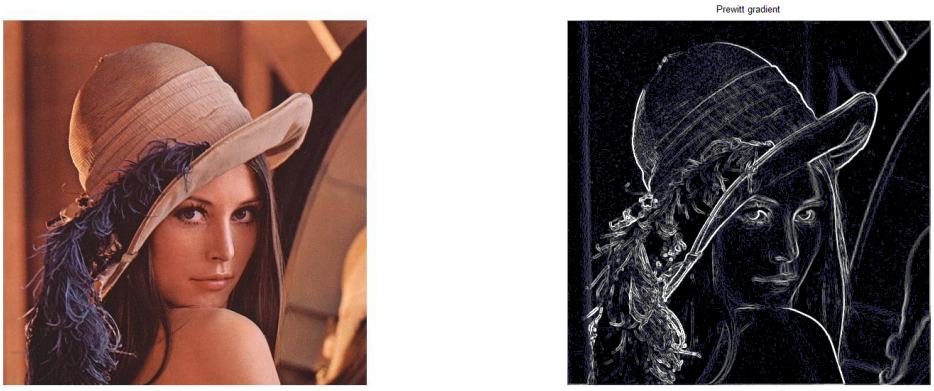

(a) (b)

Figure 6.4. (a) original Lena image **(b)** Edge detection of noiseless Lena Image using Prewitt Operator.

(a) (b)

Figure 6.5 (a) Lena image with Gaussian noise (b) Edge detection of Lena Image with Gaussian Noise using Prewitt Operator.

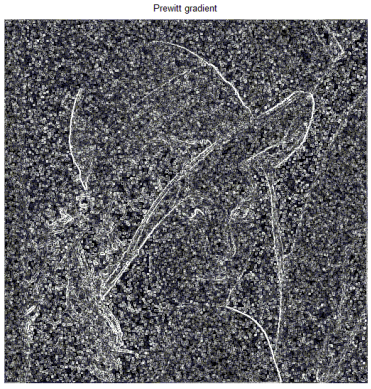

(a) (b)

Figure 6.6. (a) Lena image with Salt & Pepper noise (b) Edge detection of Lena Image with Salt & Pepper Noise using Prewitt Operator.

6.1.3 Edge Detection by using Robert Operator on noiseless and noisy Lena Image

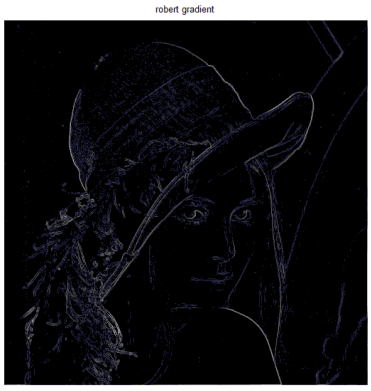

Figure 6.7. (a) original Lena image (b) Edge detection of noiseless Lena Image using Robert Operator.

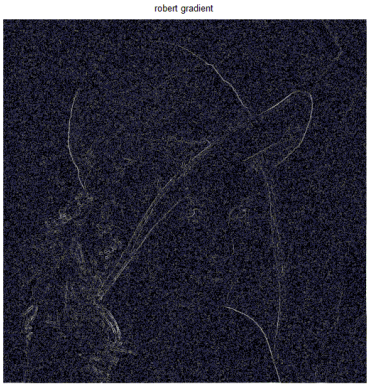

(a) (b)

Figure 6.8. (a) Lena image with Gaussian noise (b) Edge detection of Lena image with Gaussian Noise using Robert Operator.

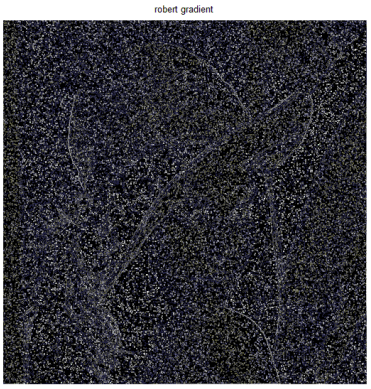

(a) (b)

Figure 6.9.(a) Lena image with Salt & Pepper noise (b) Edge detection of Lena Image with Salt & Pepper Noise using Robert Operator.

Table 6.1. Comparison of Conventional operators

OPERTOR NAME	MSE	PSNR
SOBEL	2.9580e+004	7.9551
Sobel with salt and pepper noise	3.9463e+004	5.0723
Sobel with Gaussian noise	3.5027e+004	6.2649
Prewitt	2.5821e+004	9.3141
Prewitt with salt and pepper noise	3.3283e+004	6.7754
Prewitt with Gaussian noise	2.9391e+004	8.0192
Robert	2.3322e+004	10.3320
Robert with salt and pepper noise	2.7402e+004	8.7199
Robert with Gaussian noise	2.5434e+004	9.4651

6.1.4 Edge Detection by using combination of Fractional order differential operator with Sobel Operator on noiseless and noisy Lena Image

An important property can be observed that the integer derivative is a local operator while the fractional derivative is a global operator. The fractional global operator can consider more neighboring information. Considering this characteristic, we generalize the traditional first-order Sobel edge detection operator to fractional-order for extracting image structure features.

6.1.4.1 Sobel Operator in combination with Fractional differential mask on noiseless Lena image with v= 0.1 to 0.9

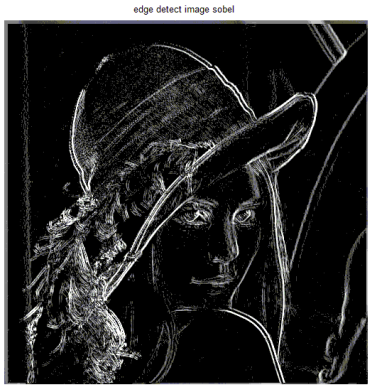

(a)

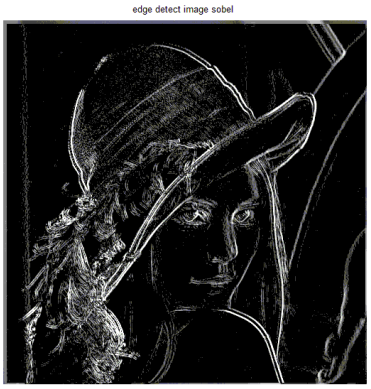

(b)

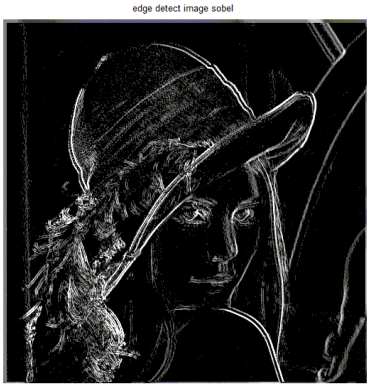

(c)

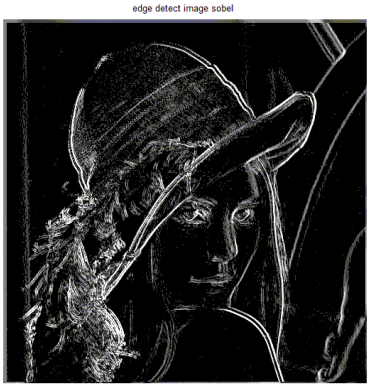

(d)

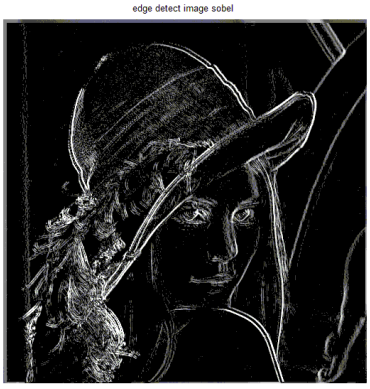

(e)

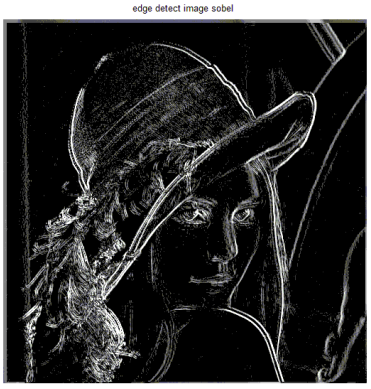

(f)

(g)

(h)

(i)

Figure 6.10. Edge detection of Lena Image with using Fractional order differential operator in combination with Sobel Operator, having order (a) v=0.1 (b) v=0.2 (c) v=0.3 (d) v=0.4 (e) v=0.5 (f) v=0.6 (g) v=0.7 (h) v=0.8 (i) v=0.9

Table 6.2 Sobel with Fractional operator

V	**MSE**	**PSNR**
0.1	2.6013e+004	9.2399
0.2	2.5742e+004	9.3447
0.3	2.5601e+004	9.3996
0.4	**2.5581e+004**	**9.4074**
0.5	2.5715e+004	9.3551
0.6	2.6093e+004	9.2092
0.7	2.6925e+004	8.8955
0.8	2.8749e+004	8.2401
0.9	3.4303e+004	6.4736

6.1.4.2 Sobel Operator in combination with Fractional differential mask on Lena image with Gaussian noise at v= 0.1 to 0.9

(a)

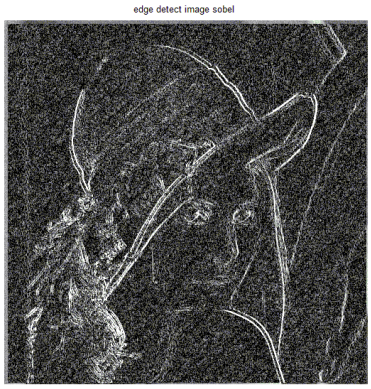

(b)

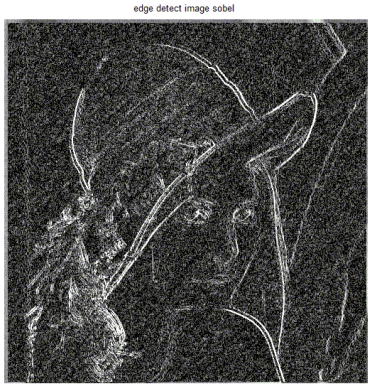

(c)

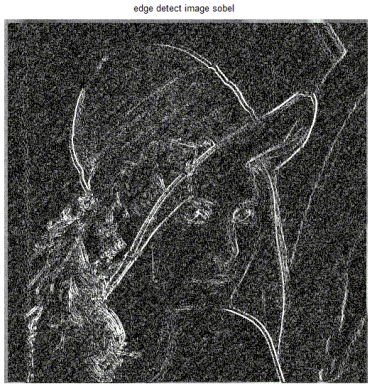

(d)

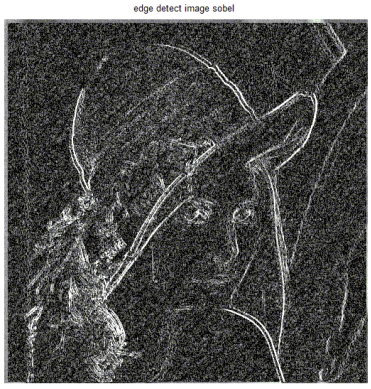

(e)

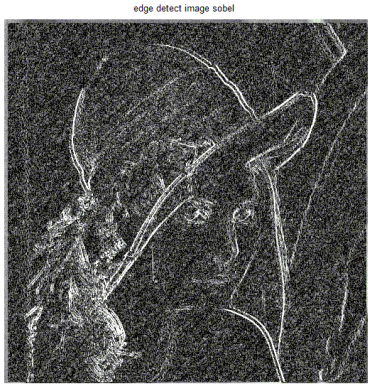

(f)

(g)

(h)

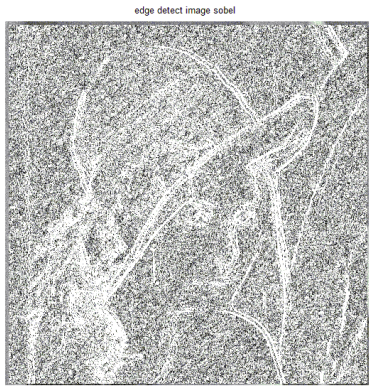

(i)

Figure 6.11. Edge detection of Lena Image with using Fractional order differential operator in combination with Sobel Operator in the presence of Gaussian noise ,having order (a) v=0.1 (b) v=0.2 (c) v=0.3 (d) v=0.4 (e) v=0.5 (f) v=0.6 (g) v=0.7 (h) v=0.8 (i) v=0.9

Table 6.3 SOBEL with FRACTIONAL operator in the presence of Gaussian noise.

V	**MSE**	**PSNR**
0.1	3.1294e+004	7.3919
0.2	3.0471e+004	7.6582
0.3	3.0010e+004	7.8105
0.4	**2.9945e+004**	**7.8325**
0.5	3.0376e+004	7.6895
0.6	3.1539e+004	7.3139
0.7	3.3870e+004	6.6007
0.8	3.8242e+004	5.3868
0.9	4.8844e+004	2.9396

6.1.4.3 Sobel Operator in combination with Fractional differential mask on Lena image with Salt & Pepper noise at v= 0.1 to 0.9

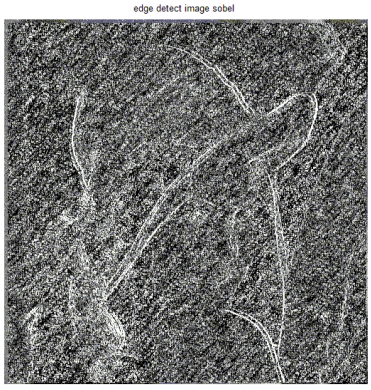

(a)

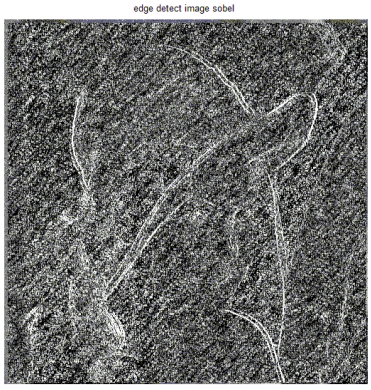

(b)

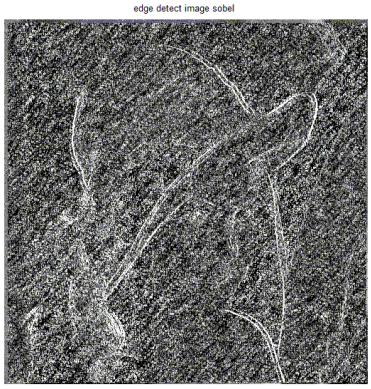

(c)

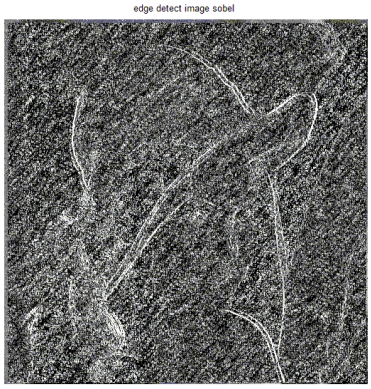

(d)

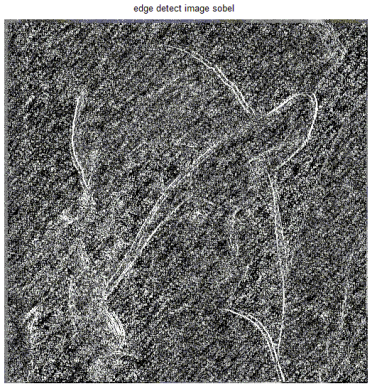

(e)

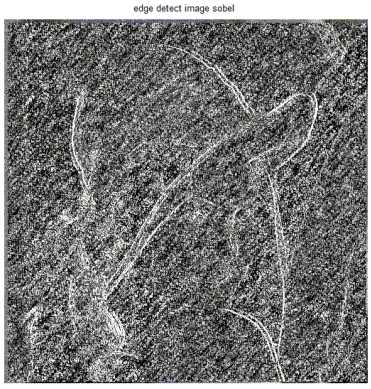

(f)

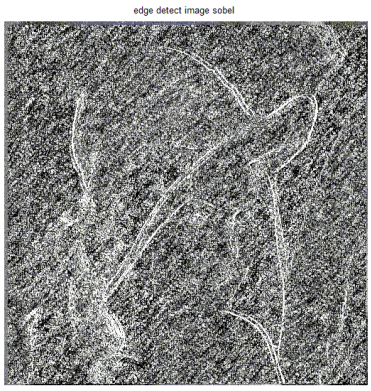

(g)

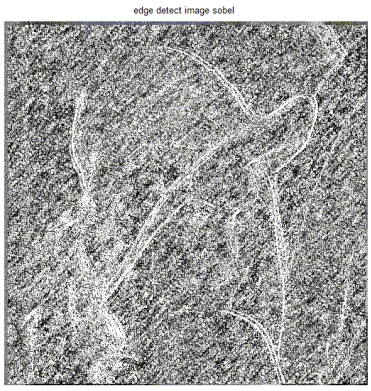

(h)

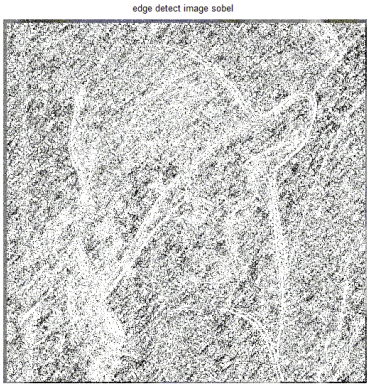

(i)

Figure 6.12. Edge detection of Lena Image with using Fractional order differential operator in combination with Sobel Operator in the presence of Salt & pepper noise having order (a) v=0.1 (b) v=0.2 (c) v=0.3 (d) v=0.4 (e) v=0.5 (f) v=0.6 (g) v=0.7 (h) v=0.8 (i) v=0.9

Table 6.4 SOBEL with FRACTIONAL operator in the presence of Salt and Pepper noise**.**

V	**MSE**	**PSNR**
0.1	3.5805e+004	6.0450
0.2	3.4807e+004	6.3278
0.3	3.4216e+004	6.4990
0.4	**3.4138e+004**	**6.5219**
0.5	3.4685e+004	6.3629
0.6	3.6091e+004	5.9656
0.7	3.8740e+004	5.2572
0.8	4.3165e+004	4.1758
0.9	5.2371e+004	2.2424

6.1.5 Edge Detection by using combination of Fractional order differential operator with Prewitt Operator on noiseless and noisy Lena Image

6.1.5.1 Prewitt Operator in combination with Fractional differential mask on noiseless Lena image with v= 0.1 to 0.9

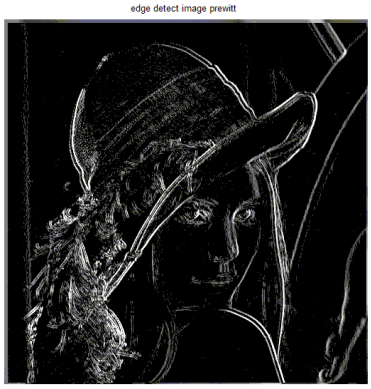

(a)

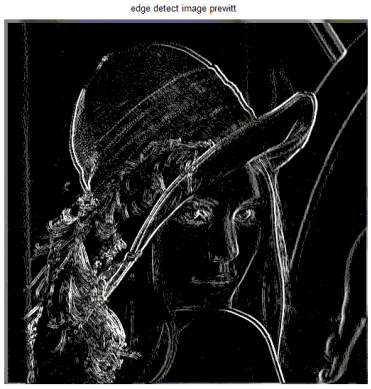

(b)

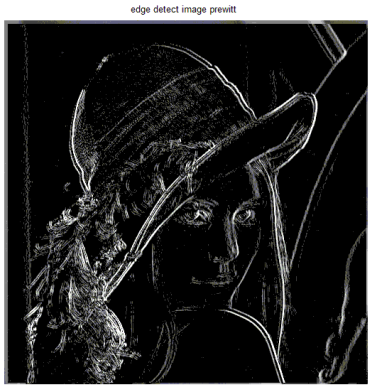

(c)

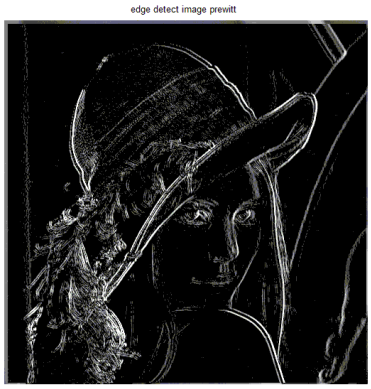

(d)

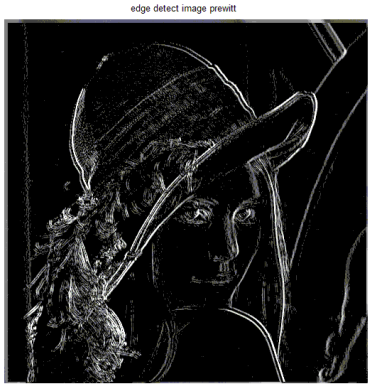

(e)

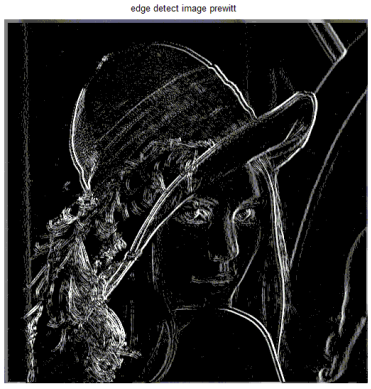

(f)

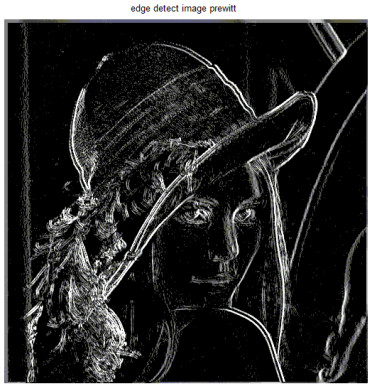

(g)

(h)

(i)

Figure 6.13. Edge detection of Lena Image with using Fractional order differential operator in combination with Prewitt Operator having order (a) v=0.1 (b) v=0.2 (c) v=0.3 (d) v=0.4 (e) v=0.5 (f) v=0.6 (g) v=0.7 (h) v=0.8 (i) v=0.9

Table 6.5 PREWITT with FRACTIONAL operator.

V	**MSE**	**PSNR**
0.1	2.5304e+004	9.5165
0.2	2.5537e+004	9.4246
0.3	2.5175e+004	9.5674
0.4	**2.5158e+004**	**9.5742**
0.5	2.5280e+004	9.5257
0.6	2.5603e+004	9.3990
0.7	2.6332e+004	9.1181
0.8	2.7948e+004	8.5226
0.9	3.2887e+004	6.8951

6.1.5.2 Prewitt Operator in combination with Fractional differential mask on Lena image with Gaussian noise at v= 0.1 to 0.9

(a)

(b)

(c)

(d)

(e)

(f)

(g)

(h)

(i)

Figure 6.14. Edge detection of Lena Image with using Fractional order differential operator in combination with Prewitt Operator in the presence of Gaussian noise ,having order (a) v=0.1 (b) v=0.2 (c) v=0.3 (d) v=0.4 (e) v=0.5 (f) v=0.6 (g) v=0.7 (h) v=0.8 (i) v=0.9

Table 6.6 PREWITT with FRACTIONAL operator in presence of Gaussian noise.

V	**MSE**	**PSNR**
0.1	2.9295e+004	8.0518
0.2	2.8623e+004	8.2840
0.3	2.8267e+004	8.4089
0.4	**2.8221e+004**	**8.4254**
0.5	2.8549e+004	8.3096
0.6	2.9517e+004	7.9765
0.7	3.1511e+004	7.3226
0.8	3.5594e+004	6.1042
0.9	4.5341e+004	3.6839

6.1.5.3 Prewitt Operator in combination with Fractional differential mask on Lena image with Salt & Pepper noise at v= 0.1 to 0.9

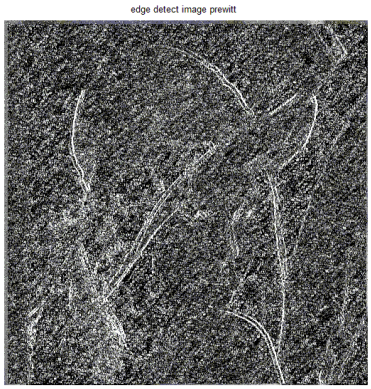

(a)

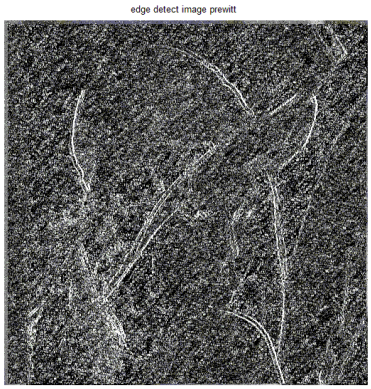

(b)

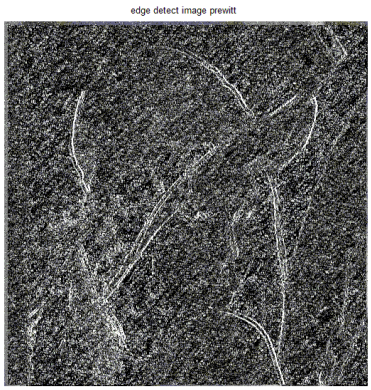

(c)

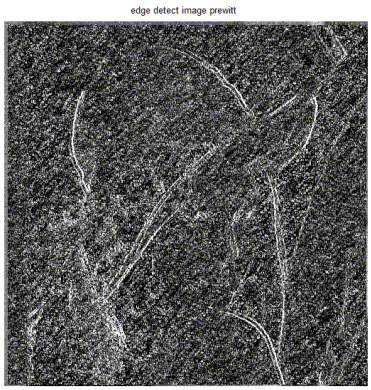

(d)

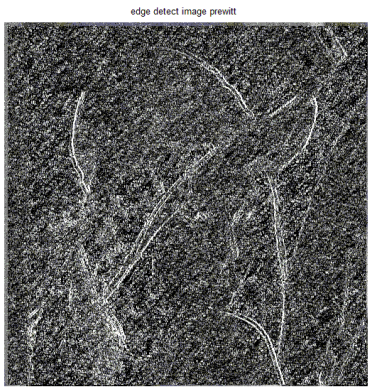

(e)

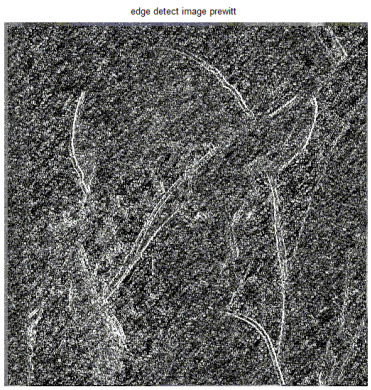

(f)

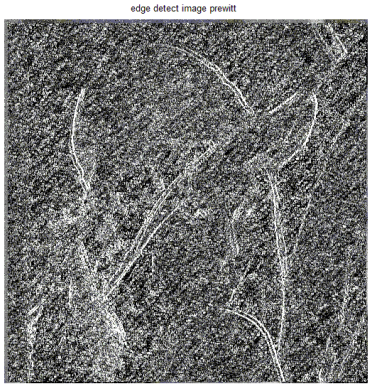

(g)

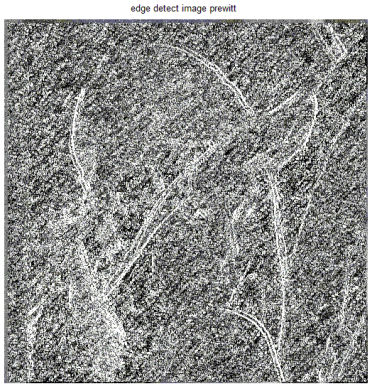

(h)

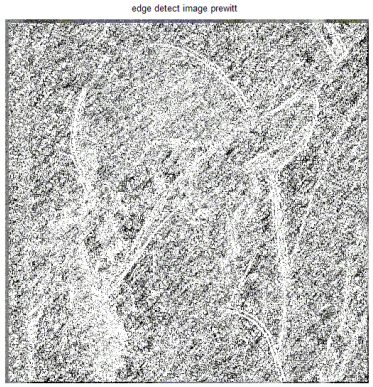

(i)

Figure 6.15. Edge detection of Lena Image with using Fractional order differential operator in combination with Prewitt Operator in the presence of Salt & pepper noise having order (a) v=0.1 (b) v=0.2 (c) v=0.3 (d) v=0.4 (e) v=0.5 (f) v=0.6 (g) v=0.7 (h) v=0.8 (i) v=0.9

Table 6.7 PREWITT with FRACTIONAL operator in presence of Salt and Pepper noise

V	**MSE**	**PSNR**
0.1	3.3542e+004	6.6981
0.2	3.2679e+004	6.9588
0.3	3.2190e+004	7.1093
0.4	**3.2151e+004**	**7.1326**
0.5	3.2586e+004	6.9872
0.6	3.3791e+004	6.6239
0.7	3.6150e+004	5.9493
0.8	4.0175e+004	4.8934
0.9	4.9964e+004	2.7129

6.1.6 Edge Detection by using combination of Fractional order differential operator with Robert Operator on noiseless and noisy Lena Image

Robert operator detects edges of an image in diagonal direction by using the difference of two adjacent pixels. Robert operator uses slash direction rather than horizontal and vertical, so edges are thin lines and are sensitive to noise. When Robert operator is combined with fractional order differential operator, it recognizes the prominent and small edges.

6.1.6.1 Robert Operator in combination with Fractional differential mask on noiseless Lena image with v= 0.1 to 0.9

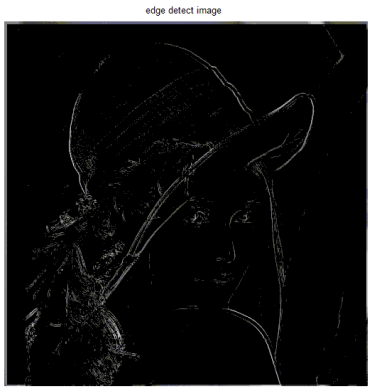

(a)

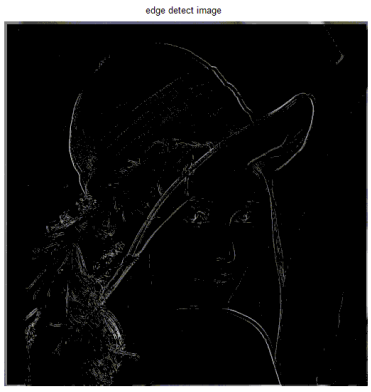

(b)

(c)

(d)

(e)

(f)

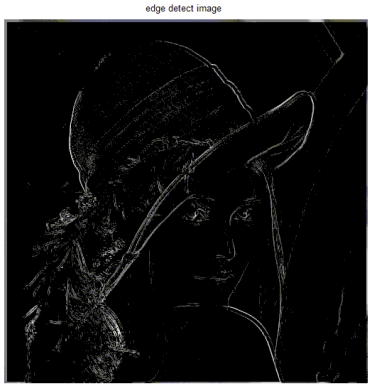

(g)

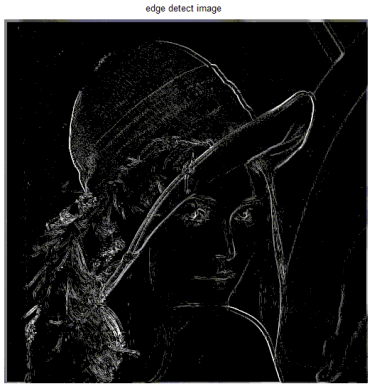

(h)

.

(i)

Figure 6.16. Edge detection of Lena Image with using Fractional order differential operator in combination with Robert Operator, having order (a) v=0.1 (b) v=0.2 (c) v=0.3 (d) v=0.4 (e) v=0.5 (f) v=0.6 (g) v=0.7 (h) v=0.8 (i) v=0.9

Table 6.8 ROBERT with FRACTIONAL operator.

V	**MSE**	**PSNR**
0.1	2.3445e+004	10.2795
0.2	2.3394e+004	10.3012
0.3	2.3369e+004	10.3117
0.4	2.3366e+004	10.4132
0.5	2.3389e+004	10.3033
0.6	2.3460e+004	10.2729
0.7	2.3635e+004	10.1985
0.8	2.4146e+004	9.9848
0.9	2.6258e+004	9.1462

6.1.6.2 Robert Operator in combination with Fractional differential mask on noiseless Lena image with Gaussian noise at v= 0.1 to 0.9

(a)

(b)

(c)

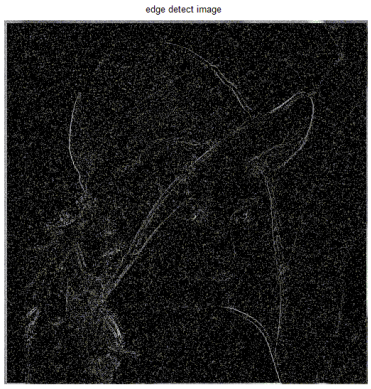

(d)

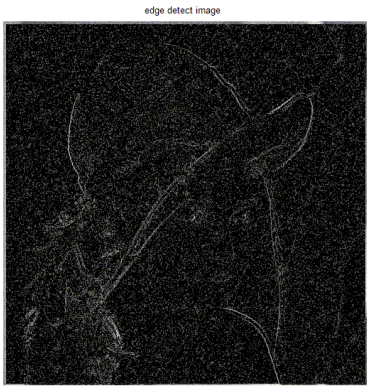

(e)

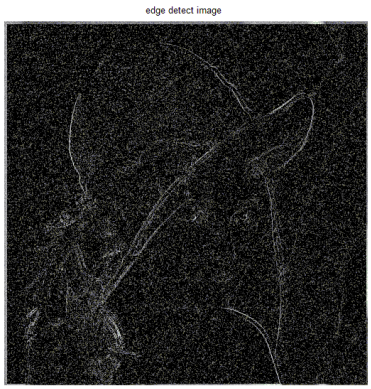

(f)

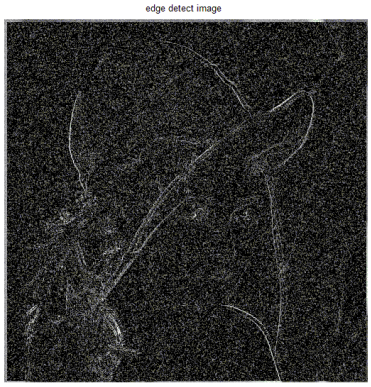

(g)

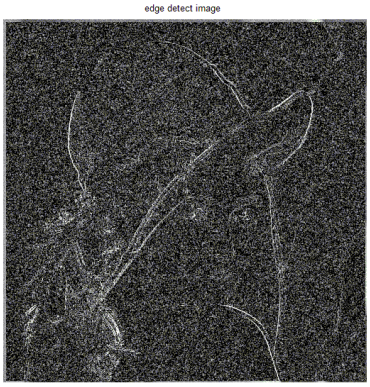

(h)

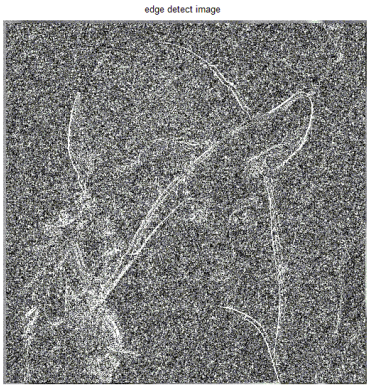

(i)

Figure 6.17. Edge detection of Lena Image with using Fractional order differential operator in combination with Robert Operator in the presence of Gaussian noise ,having order (a) v=0.1 (b) v=0.2 (c) v=0.3 (d) v=0.4 (e) v=0.5 (f) v=0.6 (g) v=0.7 (h) v=0.8 (i) v=0.9

Table 6.9 ROBERT with FRACTIONAL operator with Gaussian noise.

V	**MSE**	**PSNR**
0.1	2.5186e+004	9.5632
0.2	2.4872e+004	9.6887
0.3	2.4710e+004	9.7539
0.4	**2.4692e+004**	**9.7613**
0.5	2.4841e+004	9.7009
0.6	2.5287e+004	9.5232
0.7	2.6398e+004	9.0931
0.8	2.9496e+004	7.9834
0.9	3.8016e+004	5.4459

6.1.6.3. Robert Operator in combination with Fractional differential mask on Lena image with Salt & Pepper noise at v= 0.1 to 0.9

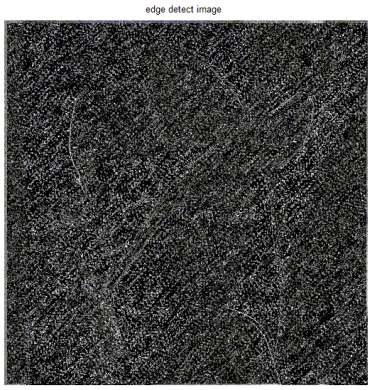

(a)

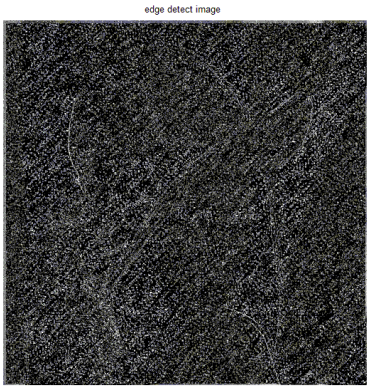

(b)

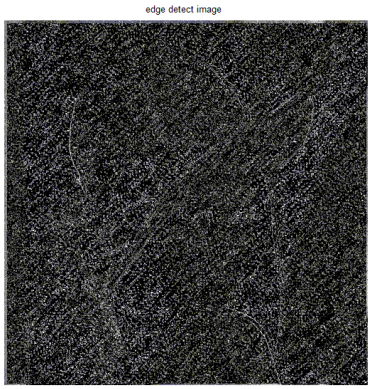

(c)

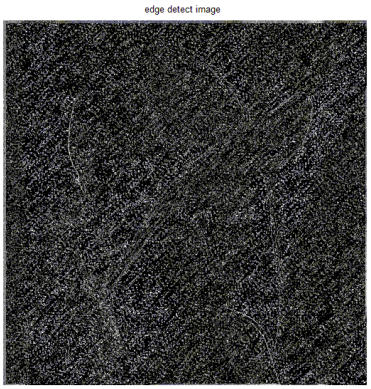

(d)

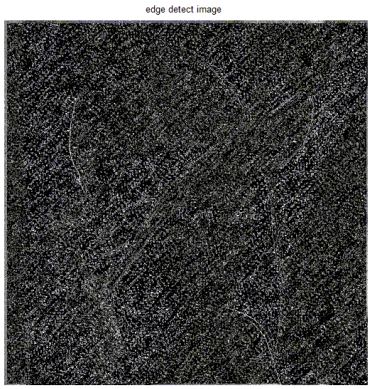

(e)

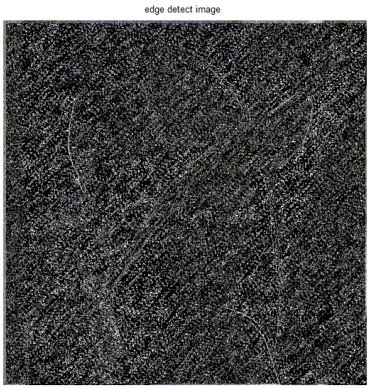

(f)

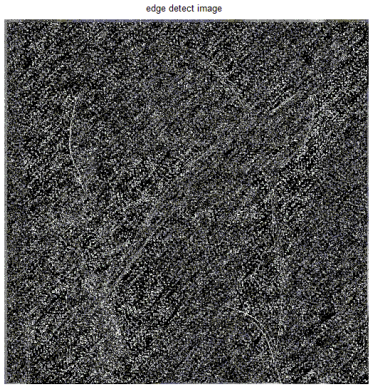

(g)

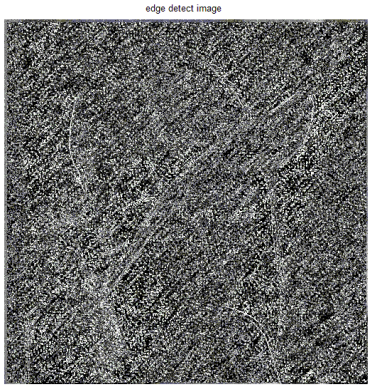

(h)

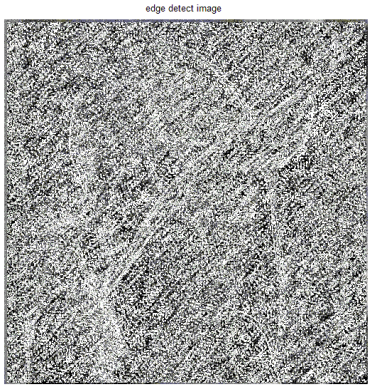

(i)

Figure 6.18. Edge detection of Lena Image with using Fractional order differential operator in combination with Robert Operator in the presence of Salt & pepper noise having order (a) v=0.1 (b) v=0.2 (c) v=0.3 (d) v=0.4 (e) v=0.5 (f) v=0.6 (g) v=0.7 (h) v=0.8 (i) v=0.9

Table 6.10 ROBERT with FRACTIONAL operator with Salt and Pepper noise.

V	**MSE**	**PSNR**
0.1	2.9151+004	8.1011
0.2	2.8528e+004	8.3172
0.3	2.8157e+004	8.4481
0.4	**2.8108e+004**	**8.4684**
0.5	2.8449e+004	8.3448
0.6	2.9341e+004	8.0363
0.7	3.1326e+004	7.4133
0.8	3.3890e+004	6.5947
0.9	4.3759e+004	4.0389

6.2 MSE and PSNR

The MSE joins corruption capacity and measurable attributes of clamor in the edge identified image. It quantifies the normal squared contrast between the estimator and the parameter. MSE indicates the normal distinction of the pixels all through the first original image with edge recognized image. The higher MSE demonstrates a more significant distinction between the original and processed image [10]. The target of way to deal with recognition, so results may differ when plotting the lines. The outstanding edge detecting operators are Sobel, Canny, Laplacian of Gaussian, Prewitt, and Roberts. These edge detection operators are exceptional in the way of magnitude, derivatives, and localization. By comparing these operators, recognized that these operators results noise level, edge relevancy and edge continuity. In commotion level, two metric models are universally used, Mean Squared Error (MSE), and Peak Signal to Noise Ratio (PSNR).

PSNR (Peak Signal-to-Noise Ratio):

The PSNR computes the peak signal to noise ratio in decibels, between two pictures [1]. This proportion is frequently utilized as quality estimation between the first and a resultant image. The higher the PSNR, the better is the nature of the yield image. To process the PSNR (6.2), we to begin with calculating the mean-squared error utilizing the additional mathematical statement:

$$MSE = \frac{1}{mn}\sum_{0}^{m-1}\sum_{0}^{n-1}\left\| f(i,j) - g(i,j)\right\|^{2} \tag{6.1}$$

$$PSNR = abs(20 * \log 10(255 / sqrt(MSE))) \tag{6.2}$$

In the above equation, m and n are the number of rows and columns in the input images, respectively where Mean Square Error (MSE) (6.1) indicates the average difference of the pixels throughout the image. A higher MSE indicates a greater difference between the original and processed image.

Chapter 7

Conclusion and Future Scope

7.1 Conclusion

In the present work, edge detection is carried out by using G-L based improved fractional differential filter. The conventional edge detection techniques suffer from various drawbacks. For instance these integral filters are susceptible to noise and in attempt edge detection edges get distorted.

Lena image is analyzed by implementing the improved G-L fractional differential filter. By varying the value of v from 0.1-0.9, we get the different results. The G-L based improved fractional differential operator detects edges more efficiently than conventional operators. When these conventional operators are compared to improved fractional differential operator, the conventional operators suffer from severe drawbacks like less degree of enhancement and more image distortion. So G-L based improved operator is used to detect and enhance the edges of an image.

A new method is used which is the combination of fractional operator with different conventional operators used. This improved operator can detect edges with high accuracy, good sharpness and with more detail. We applied new mathematical approach to improve edge detection methods by using the traditional integer order differential operators.

When the proposed masks are implemented on Lena image by increasing intensity factor and varying the order of fractional operator it gives the improved a proximity by the factor 0.4 and thus better edges of image.

Traditional integer order differential gradient operators are very sensitive to noise, while 0.4 order differential operator detects edges with relatively small noise. By applying fractional order differential operator edge detection capability of filters remains same but it somehow reduces the noise. Fractional order differential operators have strong capacity to reduce noise than integer order differential operators.

From the results of chapter (6), it examines that as the order of differential operator increases its anti-noise capacity decreases.

From the tables of PSNR it concluded that as the PSNR of operator is high, it gives the better edge extraction information. Edge detection of image by using Fractional differential operator not gives only edge but it also has good noise immunity.

From the results, it is concluded that improved fractional order differential operator detects image edges more accurately as well as by reducing the noise present in image as compared to conventional operators. It enhances the high frequency components and preserves low frequency components. The improved Fractional Differential Mask presented in this thesis work can detect the edges better than traditional operators and reduces noise.

7.2 Future Scope

The presented work can be further extended to design a Fractional Differential Filter of Digital Image using the proposed Fractional Differential Mask, and this Fractional Differential Filter can be implemented on FPGA. Also this Fractional Differential Mask can be implemented on fingerprint images, collected from the crime scene, so that there edges can be detected and enhanced.

References

[1] R. C .Gonzalez and R .E .Woods, *Digital Image Processing*, Prentice Hall, 2002.

[2] D. Ziou and S. Tabbone, Edge Detection Technique-An Overview.

[3] P. Khanzode and S. A. Ladhake, " Impulse Noise Removal Technique Based on Neural Network and Fuzzy Decisions," in *International Journal of Advanced Research in Computer Science and Software Engineering,* vol. 2, no. 2, pp. 28-32, 2012.

[4] R. Verma and J. Ali, "A Comparative Study of Various Types of Image Noise and Efficient Noise Removal Techniques," in *International Journal of Advanced Research in Computer Science and Software Engineering,* vol. 3, no. 10, pp. 617-622, 2013

[5] M. A. Farooque and J. S. Rohankar, "Survey on Various Noises and Techniques for Denoising the Color Image," in *International Journal of Application of Innovation in Engineering & Management*, vol. 2, no. 11, pp. 217-221, 2013.

[6] A. K. Boyat and B. K. Joshi, "A Review Paper: Noise Models In Digital Image Processing," in *International Journal of Signal and Image Processing*, vol. 6, no. 2, pp. 63-75, 2015.

[7] K. S. Miller and B. Ross, *An Introduction to Fractional Calculus and Fractional Differential Equation*. New York: John Wiley & Sons Inc., 1993.

[8] A. Loverro, "Fractional Calculus: History, Definitions and Application for the Engineer," report *Department of Aerospace and Mechanical Engineering,* Notre Dame, IN 46556, U.S.A, 2004.

[9] M. D. Ortigueira, " An Introduction to Fractional Continuous Time Linear Systems", in *IEEE Circuits and Systems Magazine,* vol. 8, no. 3, pp. 19-26, 2008.

[10] M. Juneja and P. S. Sandhu, "Performance Evaluation of EDGE Detection techniques for images in spatial domain," in *International Journal of Computer Theory and Engineering,* vol. 1, no. 5, pp. 1793-1820, 2009.

[11] N. Kanopoulos, N. Vasanthavada and R.L. Baker , "Design of an Image Edge Detection Filter Using the Sobel Operator," in *IEEE Journal of Solid-State Circuits*, vol. 23, no. 2, pp. 358-367, 1988.

[12] P.H. Eichel and E. J. Delp , "Quantitative Analysis of a Moment-Based Edge Operator," in *IEEE Transactions on Systems, Man, and Cybernetics*, vol. 20, no. 1, pp. 59-66, 1990.

[13] M. Gud-mundsson, E. A. El-Kwae, and M.R. Kabuka, "Edge Detection in Medical Images Using a Genetic Algorithm" in *IEEE Transactions on Medical Imaging*, vol. 17, no. 3, pp. 469-474, 1998.

[14] H. L. Tan, S.B. Gelfand and E. J. Delp, "A Cost Minimization Approach to Edge Detection Using Simulated Annealing," in *IEEE Computer Society Conference on Computer vision and Pattern recognition*, pp. 86-91, 1989.

[15] M. D. Ortigueira, "A Coherent Approach to Non-integer Order Derivatives," in *Elsevier Journal of Signal Processing,* vol. 86, no. 10, pp. 2505-2515, 2006.

[16] X. Wang, "Laplacian Operator-Based Edge Detectors," in IEEE Transactions on Pattern Analysis And Machine Intelligence, vol. 29, no. 5, pp. 886-890, 2007.

[17] H. Wechsler and M. Kidode, "A New Edge Detection Technique and its Implementation," in *IEEE Transactions on Systems, Man, and Cybernetics*, vol. 7, no. 12, pp. 827-836, 1977.

[18] I. Yasri, N. H. Hamid and V. V. Yap, "An FPGA Implementation of Gradient Based Edge Detection Algorithm Design," in *International Conference on Computer Technology and Development,* vol. 2, pp.165-169, 2009.

[19] Chun-Ling Fan and Yuan-Yuan Ren, "Study on The Edge Detection Algorithms of Road Image," in *Third International Symposium On Information Processing*, pp. 217-220, 2010.

[20] R. Harinarayan, R. Pannerselvam, M. M. Ali and D. K. Tripathi, "Feature Extraction of Digital Aerial Images by FPGA based Implementation of Edge Detection Algorithms," in *International Conference on Emerging Trends in Electrical and Computer Technology,* pp. 631-635, 2011.

[21] X. Hou and H. Liu, "Welding Image Edge Detection and Identification Research based on Canny Operator," in *International Conference on Computer Science and Service System*, pp. 250-253, 2012.

[22] V. V. Kishore and R.V.S.Satyanarayana, "Performance Evaluation of Edge Detectors –Morphology Based ROI Segmentation and Nodule Detection from

DICOM Lung Images in the Noisy Environment," in *IEEE International Advance Computing Conference*, pp. 1131-1137, 2013.

[23] Madhulika, D. Yadav, Madhurima, P. Gupta, G. Kaur, J. Singh, M. Gandhi, and A. Singh, "Implementing Edge Detection for Medical Diagnosis of a Bone in Matlab*,"* in *International Conference on Computational Intelligence and Communication Networks*, pp. 270-274, 2013.

[24] H. Yang, Y. Ye, D. Wang, and B. Jiang, "A Novel Fractional-Order Signal Processing based Edge Detection Method," in *International Conference Control, Automation, Robotics and Vision*, pp. 1122-1127, 2010.

[25] D. Tian, J. Wu and Y. Yang, "A Fractional-Order Edge Detection Operator for Medical Image Structure Feature Extraction," in *Chinese Control and Decision Conference,* pp. 5173-5176, 2014.

[26] A. Jain, M. Gupta, S. N. Tazi and Deepika, "Comparison of Edge Detectors," in *International Conference on Medical Imaging, M-Health and Emerging Communication Systems*, pp. 289-294, 2014.

[27] G. I. Chaple, R. D. Daruwala and M. S. Gofane, "Comparisons of Robert, Prewitt, Sobel Operators based Edge Detection Methods for Real Time uses on FPGA," in *International Conference on Technologies for Sustainable Development*, pp. 1-4, 2015.

[28] X. H. Chen and X. D. Fei, " Improving Edge-detection Algorithm based on Fractional Differential Approach," in *International Conference on Image, Vision and Computing*, pp. 537-542, 2012.

[29] C. Gao, J. Zhou and W. Zhang, "Edge Detection Based on the Newton Interpolation's Fractional Differentiation," in *The International Arab Journal of Information Technology*, vol. 11, no. 3, pp. 223-228, 2014.

[30] Z. J. Hou and G.W. Wei, "A New Approach to Edge Detection," in *Elsevier Journal of Pattern Recognition*, vol. 35, no. 7, pp. 1559-1570, 2002.

[31] Q. He and Z. Zhang, "A New Edge Detection Algorithm for Image corrupted by White-Gaussian Noise," in *Elsevier International Journal of Electronics and Communication*, vol. 61, no.8, pp. 546-550, 2007.

[32] Y. Zhang, Y. PU and J. Zhou, "Construction of Fractional differential Masks

Based on Riemann-Liouville Definition," in *Journal of Computational Information Systems*, vol. 6, no. 10, pp. 3191-3199, 2010.

[33] Yi. Pu, J. Zhou and X. Yuan, "Fractional Differential Mask: A Fractional Differential-Based Approach for Multiscale Texture Enhancement," in *IEEE Transactions on Image Processing*, vol. 19, no. 2, pp. 491-511, 2010.

[34] C. Gao, J. Zhou, X. Zheng and F. Lang, "Image Enhancement Based on Improved Fractional Differentiation," in *Journal of Computational Information Systems*, vol. 7, no. 1, pp. 257-264, 2011.

[35] D. Chen, C. Zheng, D. Xue And Y. Chen, "Non-Local Fractional Differential-Based Approach for Image Enhancement," in *Research Journal of Applied Sciences, Engineering and Technology*, vol. 6, no. 17, pp. 3244-3250, 2013.

[36] J. Scharcanski and A. N. Venetsanopoulos, "Edge Detection of Color Images using Directional Operators," in *IEEE Transactions on Circuits and Systems for Video Technology*, vol. 7, no. 2, pp. 397-401, 1997.

[37] H. Yang, Y. Ye, D. Wang and B. Jiang, "A Novel Fractional-Order Signal Processing based Edge Detection Method," in *International Conference Automation, Robotics And Vision*, pp. 1122-1127, 2010.

[38] M. Chakraborty, D. Maiti, A. Konar and R. Janarthanan, "A Study of the Grunwald- Letnikov Definition for Minimizing The Effects of Random Noise on Fractional Order Differential Equations," in *IEEE International Conference on Information and Automation for Sustainability*, pp. 449-456, 2008.

[39] A. J. Pinho and L. B. Almeida, "A Review on Edge Detection based on Filtering and Differentiation," *Revista Do Detua*, vol. 2, pp. 113-126, no. 1, 1997.

[40] W. K. Pratt, *Digital Image Processing*, Willy-International, 2nd Edition, 1991.

[41] M.D. Ortigueira, J.A. Tenreiro Machado and J. S. Costa, "Which differintegration?," in *IEEE proceedings- Vision, Image and Signal Processing*, vol. 152, no. 6, pp. 846-850, 2005.

[42] M. D. Ortigueira, "An Introduction to Fractional Continuous Time Linear Systems," in *IEEE Circuits and Systems Magazine*, vol. 8, no. 3, pp. 19-26, 2008.

[43] K. Diethelm, N. J. Ford, A. D. Freed and Y. Luchko, "Algorithms for the

Fractional Calculus: A Selection of Numerial Methods," in *Computer Methods in Applied Mechanics and Engineering*, vol. 194, no. 6, pp. 743-773, 2007.

[44] Y. Pu, W. Wang, J. Zhou, Y. Wang and H. Jia, "Fractional Differential Approach to Detecting Textural Features of Digital Image and its Fractional Differential Filter Implementation," in *Springer Journal of Information Sciences in China*, vol. 51, no. 9, pp. 1319-1339, 2008.

[45] Y. Pu, Z. Ji-Liu and Y. Xiao, "Fractional Differential based Approach for Multiscale Texture Enhancement," in *IEEE Transaction Image Processing*, vol. 19, no. 2, pp. 491-511, 2010.